DYNAMIC BEHAVIOUR OF AN AXIALLY MOVING MEMBRANE INTERACTING WITH THE SURROUNDING AIR AND MAKING CONTACT WITH SUPPORTING STRUCTURES

HANNU KOIVUROVA

Department of
Mechanical Engineering

OULU 1998

HANNU KOIVUROVA

DYNAMIC BEHAVIOUR OF AN AXIALLY MOVING MEMBRANE INTERACTING WITH THE SURROUNDING AIR AND MAKING CONTACT WITH SUPPORTING STRUCTURES

Academic Dissertation to be presented with the assent of The Faculty of Technology, University of Oulu, for public discussion in Raahensali (Auditorium L 10), Linnanmaa, on April 29th, 1998, at 12 noon.

OULUN YLIOPISTO, OULU 1998

Manuscript received 1 April 1998
Accepted 3 April 1998

Communicated by
Professor Pekka Neittaanmäki
Associate Professor Eero-Matti Salonen

ISBN 951-42-4949-6
(URL: http://herkules.oulu.fi/isbn9514249496/)

ALSO AVAILABLE IN PRINTED FORMAT
ISBN 951-42-4818-X
ISSN 0355-3213 (URL: http://herkules.oulu.fi/issn03553213/)

OULU UNIVERSITY LIBRARY
OULU 1998

Koivurova, Hannu, Dynamic behaviour of an axially moving membrane interacting with the surrounding air and making contact with supporting structures
Department of Mechanical Engineering, University of Oulu, FIN-90570 Oulu, Finland

Oulu, Finland
(Manuscript received 1 April 1998)

Abstract

Axially moving material problems are concerned with the dynamic response, vibration and stability of slender members which are in a state of translation. In Finland these are particularly important in the functioning of paper machines, in which out of plane vibration in the paper web, known as flutter, which from the point of view of mechanics is a phenomenon typical of an axially moving material, limits operation speeds and therefore the productivity of the machines. This subject links together a number of physical phenomena associated with aerodynamics, web movement, material behaviour and the geometry of the system. The aim of this research is to present a theoretical and numerical formulation of the nonlinear dynamic analysis of an axially moving web.

The theoretical model is based on a mixed description of the continuum problem in the context of the dynamics of initially stressed solids. Membrane elasticity is included via a finite strain model, and the membrane transport speed through a kinematical study. Hamilton's principle provides nonlinear equations which describe the three-dimensional motion of the membrane.

The incremental equations of Hamilton's principle are discretized by the finite element method. The formulation includes geometrically nonlinear effects: large displacements, variations in membrane tension and variations in transport velocity due to deformation. This novel numerical model was implemented by adding an axially moving membrane element to a FEM program which contains acoustic fluid elements and contact algorithms. This allowed analysis of problems including interaction with the surrounding air field and contact between supporting structures.

The model was tested by comparing previous experiments and present nonlinear description of the dynamic behaviour of an axially moving web. The effects of contact between finite rolls and the membrane and interaction between the surrounding air and the membrane were included in the model. The results show that nonlinearities and coupling phenomena have a considerable effect on the dynamic behaviour of the system. The nonlinearities cause a noticeable stiffening of the membrane, and the vibration frequency of nonlinear system increases as the amplitude grows. At high values of transport velocity the first mode frequency passes over the second linear harmonic, and even the third. The results also show that the cylindrical supports have a distinct influence on the behaviour of an axially moving sheet. The boundary of the contact region clearly moves and weakens the nonlinear hardening phenomena that otherwise increase the fundamental frequency. This influence strengthens as the radius of the cylinders increases.

Keywords: FEM, geometric nonlinearity, vibration, paper web

Acknowledgements

The research presented in this thesis was carried out at the Engineering Mechanics Laboratory, University of Oulu, under the supervision of Prof. Antti Pramila. His encouragement and support are greatly appreciated.

I would like to thank all my friends and colleagues at the Laboratory of Engineering Mechanics for their interest and support during the course of my work, especially Jari Laukkanen for the inspiring discussions which have many times clarified my ideas.

I am also very grateful to the reviewers of this thesis, in particular to Prof. Eero-Matti Salonen whose valuable comments and recommendations eliminated many ambiguous points from the manuscript.

The linguistic form of the English manuscript was revised by Malcolm Hicks, to whom I express my thanks for his contribution.

Financial support from the Foundation for the Promotion of Technology and Tauno Tönninki Foundation is gratefully acknowledged.

Finally, I would like to thank my wife Katariina and my sons Petteri and Antti for their patience and understanding during this time.

Oulu, 1 April 1998

Hannu Koivurova

Nomenclature

The general notation practice used here is the following. Italic letters indicate *scalars*, and with right indices they denote *tensor components*. Upper case bold letters indicate *tensors* in a three-dimensional coordinate space and lowercase bold letters indicate *vectors*. *Matrices* and *column vectors* are denoted by bold and italic letters.

Index notations

Standard tensorial notations will be used. A left superscript indicates in which configuration the quantity occurs and a left subscript shows the configuration with respect to which the quantity is measured. For example, a Green-Lagrange strain ${}^{F}_{o}\gamma_{\alpha\beta}$ at state ${}^{F}\chi$ is measured with respect to the natural state ${}^{o}\chi$. If the quantity considered occurs in the same configuration in which it is measured, the left subscript will be omitted and incremental quantities will be shown without left superscript. Right Greek letters are tensor indices reserved for surface quantities and have only the values 1, 2, while lowercase Latin indices take values 1, 2, 3 and uppercase Latin indices values from 1 to the element node number. The summation convention for repeated indices applies unless otherwise indicated.

Symbols

Definitions are given for most of the symbols in the text. The numbers of the chapters or sections describing the usage of symbols are given in parentheses.

Latin letters

A, A_o area of the cross section of a string (deformed, initial) (sec. 2.1.2)
A area of the middle surface of a membrane (chapters 3 and 4)
A vibration amplitude of the middle point of a free span (chapter 5)
A_o amplitude of the boundary motion (chapter 5)
a determinant of the metric tensor of the middle surface (chapter 3 and 4)

a_o nondimensional vibration amplitude of the middle point of a free span (sec. 5.2)
$a_{\alpha\beta}$ covariant components of the metric tensor of the middle surface (chapters 3 and 4)
$\mathbf{a}$ acceleration vector of a string particle (sec. 2.1.2)
$\mathbf{a}$ acceleration vector of a membrane particle (Appendix A)
$\mathbf{a}_\alpha$ covariant base vector of the middle surface (chapters 3 and 4)
$\boldsymbol{B}_L$, $\boldsymbol{B}_{NL}$ linear and nonlinear strain-displacement matrix (chapter 4)
b width of a membrane
$\boldsymbol{C}$ material property matrix (sec. 4.1)
$\boldsymbol{C}_f$ effective damping matrix of air (sec. 4.2)
C_u boundary curve of the fixed displacement boundary of a membrane (chapter 3)
C_σ boundary curve of the free boundary of a membrane (chapter 3)
$C^{\alpha\beta\gamma\lambda}$ components of the elasticity tensor (chapter 3 and 4)
c transverse wave speed $= \sqrt{T/m}$ (chapter 2)
c_a sound speed (sec. 2.2)
D damping coefficient (chapter 5)
$\boldsymbol{d}$ column vector of the displacement gradients (chapter 4)
E elastic modulus (chapter 2 and 5)
$\mathbf{e}_i$ unit normal base vectors (chapter 3 and 4)
$\boldsymbol{F}$ column vector of the internal force (sec. 4.1)
$\boldsymbol{F}_G$ column vector of the gyroscopic force (chapter 4.1)
$\boldsymbol{F}_f$ column vector of the fluid load (sec. 4.3)
F nondimensional frequency (chapter 5)
$\mathbf{f}$ body forces (chapter 3)
f external forces per unit length(chapter 2)
f frequency (chapter 5)
$\boldsymbol{G}$ gyroscopic inertia matrix (chapter 4)
h thickness of a membrane
$\mathbf{I}_1$, $\mathbf{I}_2$, $\mathbf{I}_3$ local base vectors of a string configuration (sec. 2.1.2)
$\boldsymbol{K}_L$ linear stiffness matrix (chapter 4)
$\boldsymbol{K}_G$ gyroscopic stiffness matrix (chapter 4)
$\boldsymbol{K}_{NL}$ geometric stiffness matrix (chapter 4)
$\boldsymbol{K}_f$ equivalent stiffness matrix of air domain (sec. 4.2)
L, l span length
$\boldsymbol{M}$ mass matrix (chapter 4)
$\boldsymbol{M}_f$ mass matrix of air domain (sec. 4.2)
m mass per unit length (chapter 2)
m_o initial mass per unit length (sec. 2.1.2)
m mass per unit area (chapter 5)
m_a added mass per unit length (sec. 2.2)
$\boldsymbol{N}$ shape function matrix (chapter 4)
N^A shape function of Ath node (chapter 4)
$\mathbf{n}$ edge force per unit length (chapter 3)
$\mathbf{n}$ outward normal vector of the fluid boundary (sec. 2.2)
$\boldsymbol{n}$ matrix of the stress components (chapter 4)
$\hat{\boldsymbol{n}}$ column vector of the stress components (chapter 4)
$n^{\alpha\beta}$ components of the Cauchy stress resultant tensor (chapter 3 and 4)

$\tilde{n}^{\alpha\beta}$ components of the second Piola-Kirchhoff stress resultant tensor (chapter 3)
P_A pressure of node A (sec. 5.2)
p surface load per unit area (chapter 3)
p pressure (sec. 2.2 and sec. 5.2)
$\boldsymbol{R}$ column vector of the external force (sec. 4.1 and 4.3)
$\boldsymbol{R}$ coupling matrix of the fluid-structure interaction (sec. 4.2)
R acoustic resistance (sec. 2.2)
r radius of supporting cylinders (sec. 5.5)
s arc length (sec.2.1.2)
T kinetic energy (chapter 3)
T normal force in string (chapter 2)
t tangential base vector in direction of θ^1 (sec. 3.2)
t, τ time
U strain energy (chapter 3)
u displacement vector of a string configuration (sec. 2.1.2)
u displacement vector of a membrane configuration (chapters 3 and 4)
$\boldsymbol{u}$ column vector of the element nodal displacements referred to fixed base $\mathbf{e}_i$ (chapter 4)
u transverse displacement (chapter 2)
u_n displacement to direction of the surface normal (sec. 2.2)
V nondimensional axial speed (chapter 5)
v, v^α transport velocity vector
$\boldsymbol{v}^2$ matrix of the transport velocity components (chapter 4)
$\hat{\boldsymbol{v}}^2$ column vector of the transport velocity components (chapter 4)
v transport speed (chapter 2)
v wave speed in air (sec. 2.2)
v_l longitudinal stiffness parameter (sec. 5.2)
v_{cr} critical transport speed $= \sqrt{n_{11}/m}$ (chapter 5)
w velocity vector of a string particle (sec. 2.1.2)
w velocity vector of a membrane particle (chapter 3)
W work of external forces (chapters 3 and 4)
W^* strain energy density (chapter 3)
x position vector of a membrane configuration (a sample point) (chapters 3 and 4)
$\boldsymbol{x}$ column vector of the element nodal coordinates referred to fixed base $\mathbf{e}_i$ (chapter 4)
x, y Cartesian coordinates

Greek letters

α parameter of added mass depending relation L/b (sec 2.2.1)
α Newmark integration parameter (chapter 4)
β parameter of added mass depending relation L/b (sec. 2.2.1)
β absorption coefficient (sec. 2.2.2)
γ amplitude decay factor (chapter 4)
$\gamma_{\alpha\beta}$ components of the Green-Lagrangen strain tensor (chapter 3 and 4)
δ variation operator (chapter 3 and 4)

δ Newmark integration parameter (chapter 4)
$\boldsymbol{\varepsilon}$ column vector of the linear strain (chapter 4)
ε perturbation coefficient (sec. 5.2)
$\varepsilon_{\alpha\beta}$ components of linear part of the Green-Lagrangen strain tensor (chapters 3 and 4)
$\eta_{\alpha\beta}$ components of nonlinear part of the Green-Lagrangen strain tensor (chapters 3 and 4)
∇ nabla operator (chapter 3)
θ^{α} components of the convected coordinates of a membrane configuration (chapters 3 and 4)
κ curvature of coordinate curve θ^1 (sec. 3.2)
Λ span length after Galileo and Lorenz transformation (sec. 2.4)
μ friction coefficient (sec. 5.5)
ρ mass density of a membrane
ρ_a air density (sec. 2.2)
$\mathfrak{v}$ unit normal vector of the membrane boundary (chapter 3)
χ configuration of a string (sec. 2.1.2)
χ configuration of a membrane (chapters 3 and 4)
ω angular frequency

Notations of differentiation

Partial derivatives respect to convected coordinates θ^{α} will be denoted to the following two ways

$$\frac{\partial x}{\partial \theta^{\alpha}} = x,_{\alpha}$$

and similar notations will be used with the time derivatives

$$\frac{dx}{dt} = x,_{t}$$

Contents

1. Introduction

The productivity of paper machines is limited due to maximum operating speeds, since building even wider machines is no longer profitable. One of the most serious obstacles to high speed operation has been web flutter (vibrations) which causes quality problems or breaks in the web. The flutter problem in paper machines producing lightweight papers can be serious in or near the dryer section, where the paper web has to pass over a span without a supporting wire, felt or conveying band. The problem will be solved in new paper machine constructions by escorting paper web over the critical locations with a felt or conveyor belt. The operating speed will increase, but the flutter phenomenon and the need for a good knowledge of it will not decrease. On the contrary, the dynamic behaviour of wires, felts and conveyor belts and of flutter of the paper web in places where escorting is impossible will become even more critical.

From the point of view of mechanics, the out of plane vibration, or flutter, is a typical phenomenon of axially moving material, encompassing systems such as pipes containing flowing fluid, moving strings and belts, high speed magnetic tapes, printing presses etc. Recent developments in research into axially moving materials are reviewed by Wickert & Mote (1988), Arbate (1992) and Païdoussis & Li (1993). A paper sheet is a good example of a thin membrane which is in a state of translation. The subject is a well-known one as far as linear cases are concerned. The first analyses of the flutter of a moving web were performed using analytical "travelling thread line" models (Mujumdar & Douglas 1976, Pramila 1986,1987). The cross direction variation in web motion was neglected by assuming that the entire web width deflects uniformly, and the surrounding air was modelled as an added mass. The importance of the surrounding air for light webs was noticed at that stage, however, and it was shown to affect the natural frequencies and critical speed of the web. Later a web was modelled as a linear membrane and the surrounding air with an incompressible (Niemi & Pramila 1987) or compressible fluid model (Laukkanen & Pramila 1997).

To cope with flutter problems, we need to identify the causes and mechanisms of flutter. Despite numerous studies there is no consensus about the main causes, and the mechanisms are not clearly understood. This subject couples several distinct physical phenomena associated with aerodynamics, web movement, material behaviour and the geometry of the system. (Chang 1990). Simple linear models are not enough, and there is a need for more complicated models which combine these physical phenomena and include nonlinear effects

(Wickert 1992).

The objective of this paper is to present a nonlinear theoretical model for a prestressed, axially moving membrane, including the effects of large deflections, variation in tension along the membrane and variation in transport velocity due to deformation. Incremental equations are developed in the same way as in the analysis of prestressed elastic structures outlined by Reismann & Pawlik (1977) for hyperelastic solids and applied by Luongo *et al*. (1984) to an elastic cable and by Perkins & Mote (1987) to a travelling cable. Membrane elasticity is included via a finite strain model and the membrane transport speed through a kinematical study, which, with the convected coordinate, allows variation in transport motion to be considered as well. The equations of motion are developed using Hamilton's principle. The general theory of an axially moving arbitrary membrane is applied to two theoretical applications: an axially moving web passing over two finite supporting cylinders, and an initially plane axially moving web between fixed simple supports.

A numerical formulation based on finite element analysis (FEM) is presented that includes the above capabilities. This is implemented into a commercial FEM program which contains acoustic fluid elements and contact algorithms. Hence analyses of problems containing interaction with a surrounding air field and contact between supporting structures are possible. A numerical model is used to estimate the influence of geometrically nonlinear effects, contact and surrounding air on the dynamic behaviour of the axially moving membrane.

2. Background to the phenomena and system considered

2.1. Axially moving material

2.1.1. Characteristics of axially moving material

The problem of axially moving materials is an extensive one that encompasses such apparently diverse mechanical systems as the paper web in a paper mill or printing press, on/off winding of textile fibers and paper, filament winding of composite components, high speed magnetic tapes, power transmission chains and belts, band saws, pipes conveying fluid etc. Vibration is generally undesirable in such systems, but it is characteristic of operation at high transport speeds. Transverse motion in wide band saw blades, for instance, results in poor cutting quality and increased residuals. For tape drives that operate in a longitudinal recording format, vibration of the tape against the recording head accelerates wear and modulates the recorded or replayed signal.

The following typical features dominate the dynamic response of an axially moving material in the linear range (Wickert & Mote 1991).

(1) Disturbances travel at different speeds in the upstream and downstream directions. In the upstream direction the wave propagation speed is the difference between the transport speed v and the wave propagation speed in a nonmoving structure c, $v - c$, while downstream these are summed $v + c$. (Fig. 1a).

(2) Transverse vibration does not have a constant spatial phase, and therefore material particles pass through the equilibrium at different times, see Fig. 2. The phase shift becomes more visible as the transport velocity increases.

(3) Natural frequencies decrease monotonically with speed, and reach zero at the critical value where $v = c$ (see Fig. 3). This happens because the propagation of disturbances upstream stops and divergence instability occurs. With a travelling string, all its natural frequencies vanish at the same speed, but with a travelling beam the natural frequencies vanish at their own critical speeds because of dispersion.

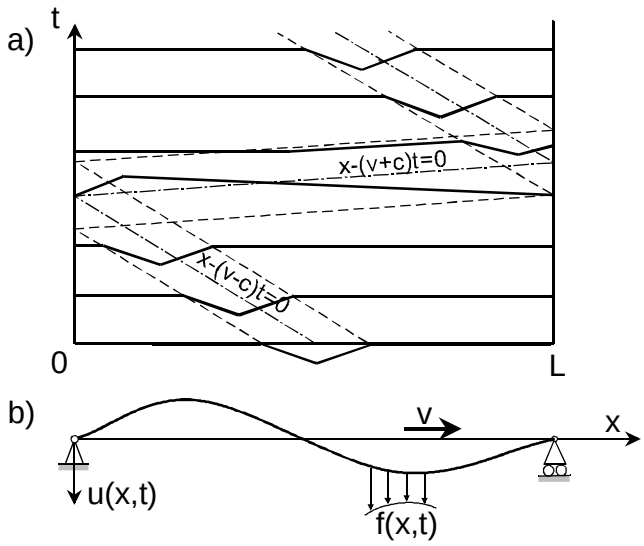

Fig. 1. a) Propagation of a disturbance in an axially moving material (Lee 1968). b) Model of an axially moving string.

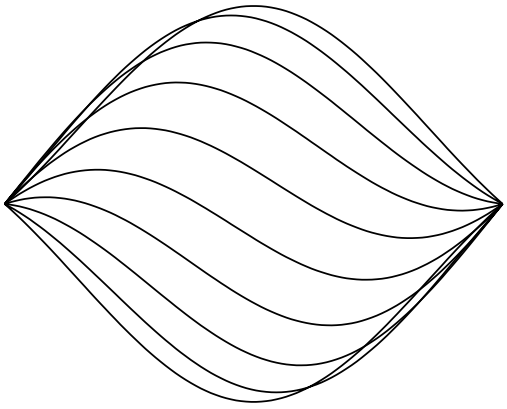

Fig. 2. Fundamental mode of a travelling string over a half period of motion.

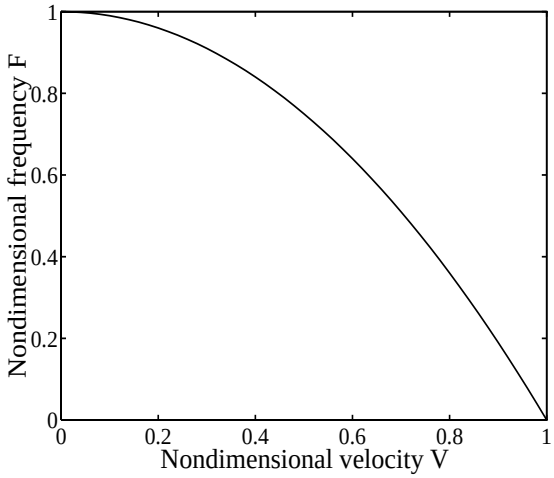

Fig. 3. Fundamental frequency of a travelling string as a function of transport speed.

(4) The stability of an axially moving structure can be lost in three characteristic ways
- divergence instability at the critical speed,
- flutter instability at a speed above the critical value, and
- Mathieu-type instability due to parametric excitation.

From a mathematical standpoint, the above characteristics arise from Coriolis and centripetal inertia terms in the equation of motion which force the eigenfunctions to be complex. For instance the equation of motion of a travelling tensioned string shown in Fig. 1b is

$$m u_{,tt} + 2 m v u_{,xt} + m\left(v^2 - c^2\right) u_{,xx} = f, \tag{2.1}$$

where u is the transverse displacement, m is the mass per unit length, v is the transport speed and c is the wave propagation speed of a string which is square of tension force T per mass m or $\sqrt{T/m}$. The transverse displacement $u(x,t)$ is measured in the Eulerian sense, and the material particles experience the local $mu_{,tt}$, Coriolis $2mv\,u_{,xt}$ and centripetal $mv^2\,u_{,xx}$ acceleration components in location x at the time t. Other terms in equation (2.1) are the effect of a normal force $Tu_{,xx}$ and the external forces per unit length f. Although there is a single temporal derivative of displacement in the Coriolis term suggesting viscous damping, the model includes no dissipation.

There are two obvious shortcomings in the linear theory, which become still more apparent with increasing transport speed. First, the linear theory does not take into consideration the geometrical nonlinearities: tension variation due to transverse displacement and the effect of variations in transport velocity due to deformation. Especially

at near-critical speeds, where the modal stiffness is small, these nonlinear elements dominate the dynamic response. (see Fig. 4). In general, the linear theory underestimates stability in the subcritical range, overestimates it for supercritical speeds and is most limited in a near-critical regime (Wickert 1992).

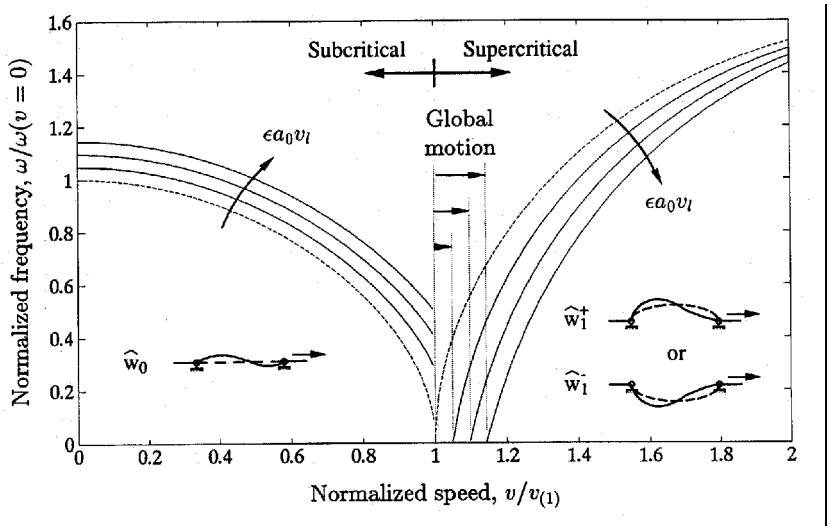

Fig. 4. Fundamental frequency of a travelling beam as a function of transport speed with a linear (-----) and a nonlinear (———) theory, where ε is the perturbation coefficient, a_o is a amplitude and v_l is stiffness parameter (Wickert 1992).

Secondly, a linear theory cannot describe bifurcation from the straight configuration to curved equilibrium states in a supercritical transport speed regime, nor local motion about the equilibrium or global motion between coexisting equilibria. In practice sudden bifurcation will hardly be detected, as it happens smoothly from straight to curved with the increase of transport speed (Wickert 1992).

The above conclusions are valid for a model of a taut geometrically perfect (straight) axially moving material. In some applications, however, the effect of a geometrical error arising from initial curvature, for instance, cannot be eliminated by system tension. Sources of initial curvature include bending moments generated by supporting wheels and pulleys, sag due to gravity, material imperfections and guide misalignment. Although these imperfections are usually small, they can play a dominant role in the dynamic response of a system (Hwang & Perkins 1992a). For flexible materials, such as cables, initial curvature due to gravity sag leads to a stabilizing "speed-tensioning effect" (Perkins & Mote 1989). This means that the curved equilibrium state does not have "a critical speed" at all as the taut string model would predict. There also exists another equilibrium state in which the element may stand up vertically in the shape of an arch. Both theory and experiment demonstrate that this arch-like equilibrium can also be stabilized at sufficiently high

translation speeds (Perkins & Mote 1989, Perkins 1989).

The consideration of systems including flexural stiffness differs in some sense from the above. In these systems the initial curvature arises from the bending of a structure about the guiding structure, pulleys or wheels. Bending of the geometry leads to a single non-trivial curved equilibrium at subcritical speeds, which bifurcates to multiple curved equilibrium states in a supercritical speed region. The results of Hwang & Perkins (1992b) show that critical speed behaviour for axially moving materials is extremely sensitive to system imperfections such as initial curvature. When there is any degree of initial curvature, no divergence instability exists at the traditional fundamental "critical" speed (Hwang & Perkins 1992a, 1992b).

2.1.2. Nonlinear formulations for the travelling string problem

The earliest nonlinear theoretical studies were those of Zaiser (1964) for analyzing the travelling string problem using a Eulerian description. He began from an application of Newton's second law to control volume and obtained four simultaneous differential equations for the axial momentum, transverse momentum, mass tension relation and continuity:

$$
\begin{aligned}
& m\left(v^x v^x_{,x} + v^x_{,t}\right) = \frac{1}{\sqrt{1 + u_{,x}^2}} \frac{\partial}{\partial x}\left\{\frac{T}{\sqrt{1 + u_{,x}^2}}\right\} \\
& m\left(u_{,tt} + 2 v^x u_{,xt} + \left(v^x\right)^2 u_{,xx}\right) = \frac{T u_{,xx}}{1 + u_{,x}^2} \\
& T = E A_o\left(\frac{m_o}{m} - 1\right) \\
& \frac{\partial}{\partial x}\left(m v^x \sqrt{1 + u_{,x}^2}\right) + \frac{\partial}{\partial t}\left(m \sqrt{1 + u_{,x}^2}\right) = 0
\end{aligned}
\qquad (2.2)
$$

where v^x is the x component of transport velocity, A_o is the initial cross-section area of the cable, m_o is the mass per unit length in the initial state and m is the mass per unit length in the deformed state. Ames *et al.* (1968) and Kim & Tabarrok (1972) later derived similar formulations. The nonlinear model includes the effects of transport velocity, tension and mass variations and geometric nonlinearities.

Mote (1966) developed an alternative formulation that included the elastic effect and geometric nonlinearity by means of Hamilton's principle. The transport velocity was taken as a constant. In a further derivation he assumed the derivatives of longitudinal displacement to be small and ignored them. This led to a second-order equation, the transverse equation of motion. Later Thurman & Mote (1969) and Wickert (1992) used

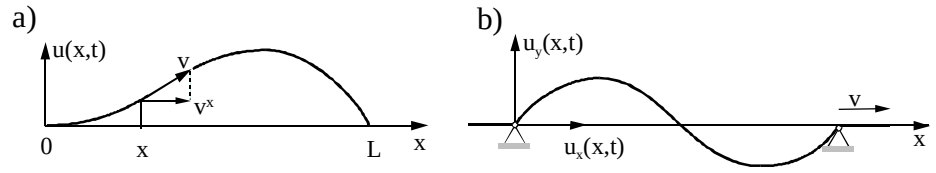

Fig. 5. Schematic models for axial moving string formulations. a) Eulerian description (Ames *et al.* 1969). b) "Mixed" description (Wickert 1992).

same kind of formulation without the assumption for derivatives of longitudinal displacement, resulting in a governing equation for longitudinal and transverse motion:

$$\begin{aligned} m\left(u^{x}_{,tt} + 2\,v\,u^{x}_{,xt} + v^2\,u^{x}_{,xx}\right) - EA\,\frac{\partial}{\partial x}\left(u^{x}_{,x} + \tfrac{1}{2}\left(u^{y}_{,x}\right)^2\right) &= 0 \\ m\left(u^{y}_{,tt} + 2\,v\,u^{y}_{,xt} + v^2\,u^{y}_{,xx}\right) - \frac{\partial}{\partial x}\left(\left[T + EA\left(u^{x}_{,x} + \tfrac{1}{2}\left(u^{y}_{,x}\right)^2\right)\right]u^{y}_{,x}\right) &= 0\ . \end{aligned} \tag{2.3}$$

The most notable difference between these two developments is the definition of displacement (see Fig. 5). Zaiser (1964) and Ames *et al.* (1968) used a pure Eulerian frame, which they define the displacement u of a particle of a string with respect to a spatial point x. Mote (1966), Thurman & Mote (1969) and Wickert (1992) used a kind of mixed description, defining a transverse displacement u^{y} (displacement in a Eulerian frame) and a longitudinal displacement u^{x}, which according to Mote (1966) is related to coordinates translating at velocity v. Wickert (1992) later corrected this by describing the longitudinal displacement as well in the spatial frame. Moreover, he added that longitudinal and transverse displacement must be coupled for finite amplitude motion. Thurman & Mote (1968) did not comment on the description of longitudinal displacement or its definition in their paper at all. From the above development of the equations of motion we can come to the conclusion that the definition of longitudinal displacement is "a shortcut" to a simpler formulation of the strain energy needed in Hamilton's principle. Since strain energy can actually be written in the same form as a non-moving string, nonlinear geometric behaviour is easy to add to the model, and the resulting governing equations (2.3) are easier to solve than equations (2.2), which come from the pure Eulerian description.

An even more "advanced" formulation of this kind is presented by Perkins & Mote (1987), who consider the vibration of a travelling elastic cable (a loose string). The state of equilibrium (steady state) is not straight as it is in the problem of an axially moving string and the definition of displacement used is not valid. Perkins & Mote (1987) defined displacement as a vector from a so-called equilibrium configuration to a final configuration (see Fig. 6). The displacement vector is said to "represent the three-dimensional motion of the final configuration, and it is distinguished from the motion of a cable particle which includes the particle transport velocity", meaning that the velocity of a particle at the point

${}^{F}P$, denoted ${}^{F}\mathbf{w}$, consists of the movement of the configuration $\mathbf{u}$ and the transport motion ${}^{F}\mathbf{v}$

$$ {}^{F}\mathbf{w} = \mathbf{u}_{,t} + {}^{F}\mathbf{v} \ . \tag{2.4} $$

In the same way as above, the description simplifies the strain energy of a travelling cable to the form of a non-moving cable.

Since Perkins & Mote (1987) did not present all the details of their formulation, some of them will be interpreted below according to Salonen (1998). The main problems in this formulation are the definition of motion through displacement of the configuration and the association of a point in the configuration with a passing material particle. The association can be explained as follows. First we designate the points of different configurations under consideration ${}^{o}0$, ${}^{I}0$ and ${}^{F}0$ as sample points, meaning that we imagine that the cable of states ${}^{I}\chi$ and ${}^{F}\chi$ is cut off from its supports A and B and if the pieces of cable are placed on a "frictionless table" next to the base cable ${}^{o}\chi$, shown in Fig. 6, the particles at the points ${}^{I}0$ and ${}^{F}0$ will lie at the distance ${}^{o}s$ from the support A after removal of the stresses. This assumption requires that a detached piece is a "clone" of the base cable ${}^{o}\chi$ at an arbitrary moment having the same number of material particles, which are also distributed in the same way. As a result it can be concluded that the flow of material particles should be homogeneous in order to comply with the above assumption.

The second detail to consider is the derivation of the equation of transport velocity in the final configuration

$$ {}^{F}v \ {}^{F}\mathbf{I}_1 = {}^{I}v\left[\mathbf{I}_1 + u\left({}^{I}s,t\right)_{,s}\right] . \tag{2.5} $$

Here $(\,)_{,s}$ denotes partial differentiation with respect to ${}^{I}s$. Perkins & Mote (1987) used the equation of the local tangential base vector in the final configuration

$$ {}^{F}\mathbf{I}_1 = \left[\mathbf{I}_1 + u\left({}^{I}s,t\right)_{,s}\right] \mathrm{d}\,{}^{I}s \,/\, \mathrm{d}\,{}^{F}s \tag{2.6} $$

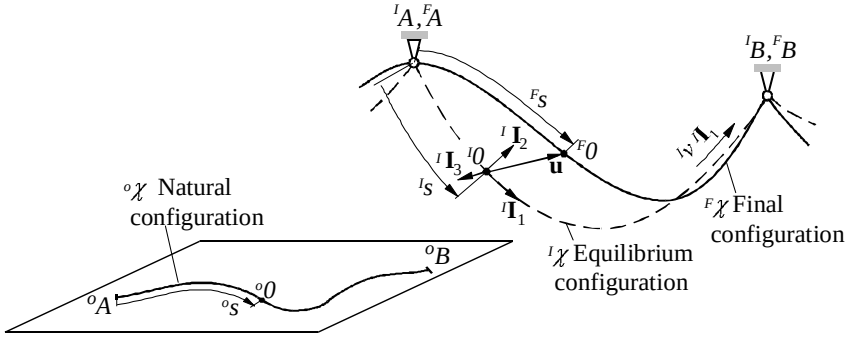

Fig. 6. Definition diagram for the natural, equilibrium and final configurations of a cable and the displacement in a point of the configuration (Perkins & Mote 1987, Salonen 1998).

and two equations of mass conservation

$$\mathrm{d}\,{}^{I}s\;{}^{I}A = \mathrm{d}\,{}^{F}s\;{}^{F}A \tag{2.7}$$

and

$${}^{I}A\;{}^{I}v = {}^{F}A\;{}^{F}v \tag{2.8}$$

to form the equation (2.5). The first equation of mass conservation is obvious (if the density is a constant), but it is unclear how they arrived at the second one. Salonen (1998) showed that the equation (2.5) can be developed using the kinematics of the cable alone.

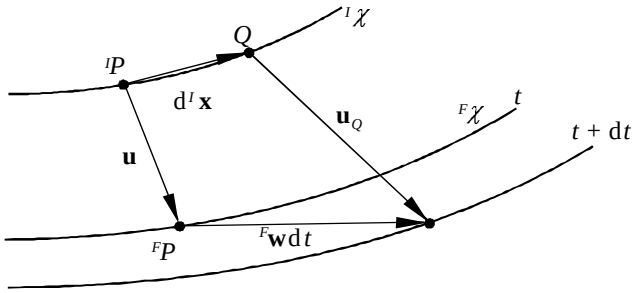

Fig. 7. Displacement of a point in the configuration, and movement of a material particle, after Salonen (1998).

The motion of a particle is followed during a short time step dt from the point ${}^{I}P$ in the steady state and from the corresponding sample point ${}^{F}P$ in the final state, shown in Fig. 7. The displacement of a particle in the steady state consists of transport motion only and is therefore

$$\mathrm{d}\,{}^{I}\mathbf{x} = {}^{I}\mathbf{v}\,\mathrm{d}t\ . \tag{2.9}$$

The displacement of a particle from the final state consists of the transport motion and the motion of configuration, according to (2.4), and is now ${}^{F}\mathbf{w}\ \mathrm{d}t$. The displacement of the sample point ${}^{I}P$, the point in the configuration where particle is located at time t, is $\mathbf{u} = \mathbf{u}\,({}^{I}s, t)$, thus ${}^{I}s$ and t are used as independent variables. The displacement of a configuration point Q where the particle under examination is located at time $t + \mathrm{d}t$ is therefore

$$\begin{aligned} \mathbf{u}_Q &= \mathbf{u} + \mathrm{d}\,\mathbf{u} = \mathbf{u} + \mathbf{u}_{,s}\,\mathrm{d}\,{}^{I}s + \mathbf{u}_{,t}\,\mathrm{d}t \\ &= \mathbf{u} + \mathbf{u}_{,s}\,{}^{I}v\,\mathrm{d}t + \mathbf{u}_{,t}\,\mathrm{d}t\ . \end{aligned} \tag{2.10}$$

The result was obtained by means of the chain rule and a scalar version of equation (2.9), or $\mathrm{d}^I s = {}^I v\, \mathrm{d}t$. Finally, if we use the geometry of Fig. 7, develop a vector equation

$$\mathbf{u} + {}^F\mathbf{w}\,\mathrm{d}t = \mathrm{d}\,{}^I\mathbf{x} + \mathbf{u}_Q \ . \tag{2.11}$$

and substitute equations (2.4), (2.9) and (2.10) into it, the expected result is obtained:

$${}^F\mathbf{v} = {}^I\mathbf{v} + {}^I v\,\mathbf{u}_{,s} = {}^I v\left({}^I\mathbf{I}_1 + \mathbf{u}_{,s}\right) . \tag{2.12}$$

Applying equation (2.6), we obtain the transformation equation in the form

$${}^F\mathbf{v} = {}^I v\,\frac{\mathrm{d}\,{}^F s}{\mathrm{d}\,{}^I s}\,{}^F\mathbf{I}_1 = {}^F v\ {}^F\mathbf{I}_1 \ , \tag{2.13}$$

which shows that the transport velocity does indeed operate in a direction tangential the final configuration, which, taken together with the first equation of mass conservation (2.7), results in the second equation of mass conservation. Actually, we can see that the equations (2.5) and (2.13) are consequences of kinematics only, and that the second equation of mass conservation follows from them and not vice versa.

The acceleration of a particle in the cable can be developed from the change in velocity using the chain rule, a scalar version of equation (2.9) and equation (2.4), i.e.

$$\begin{aligned} \mathrm{d}\,{}^F\mathbf{w} &= {}^F\mathbf{w}_{,s}\,\mathrm{d}\,{}^I s + {}^F\mathbf{w}_{,t}\,\mathrm{d}t \\ &= {}^F\mathbf{w}_{,s}\,{}^I v\,\mathrm{d}t + {}^F\mathbf{w}_{,t}\,\mathrm{d}t \\ &= \left(\mathbf{u}_{,ts} + {}^F\mathbf{v}_{,s}\right){}^I v\,\mathrm{d}t + \left(\mathbf{u}_{,tt} + {}^F\mathbf{v}_{,t}\right)\mathrm{d}t \ . \end{aligned} \tag{2.14}$$

Thus, if we divide the change in velocity by $\mathrm{d}t$ and substitute (2.5), we obtain the acceleration vector

$$\begin{aligned} {}^F\mathbf{a} &= \frac{\mathrm{d}\,{}^F\mathbf{w}}{\mathrm{d}t} = \mathbf{u}_{,tt} + {}^I v\,\mathbf{u}_{,st} + {}^F\mathbf{v}_{,t} + {}^I v\ {}^F\mathbf{v}_{,s} \\ &= \mathbf{u}_{,tt} + {}^I v\,\mathbf{u}_{,st} + \left[{}^I v\left({}^I\mathbf{I}_1 + \mathbf{u}_{,s}\right)\right]_{,t} + {}^I v\left[{}^I v\left({}^I\mathbf{I}_1 + \mathbf{u}_{,s}\right)\right]_{,s} \ . \end{aligned} \tag{2.15}$$

By reducing this equation and substituting the component form of the displacement $\mathbf{u} = u_1\,{}^I\mathbf{I}_1 + u_2\,{}^I\mathbf{I}_2 + u_3\,{}^I\mathbf{I}_3$ into it, we obtain the same inertia terms as in the equations of motion in the paper of Perkins & Mote (1987).

The formulation considered above is also used to develop a theoretical model for an axially moving membrane, presumably for the same reason as above, the possibility for modelling the elasticity of the membrane and the travelling motion in a straightforward manner, leading to simpler equations.

2.2. The surrounding air

Theoretical and experimental results show that the effect of the surrounding air on the dynamic behaviour of a paper web is significant. According to Pramila's (1986) "threadline" model and experimental results the critical velocities and natural frequencies are only 15 – 30% of the values given by predictions that neglect the interaction between the paper sheet and surrounding air (Fig. 21 on page 62). Three dimensional finite element analysis also shows that the shape of the free air field has a considerable influence on the dynamic response, and that this increases with an increase in the width/length ratio of the web (Niemi & Pramila 1987, Laukkanen & Pramila 1997).

2.2.1. Added mass

In theoretical considerations the simplest approach for taking account of the flow around a vibrating structure is potential flow idealization. This means that the surrounding air is assumed to be incompressible and non-viscous, and its flow is assumed to be irrotational. These assumptions are fulfilled most notably at the transverse vibration frequencies of a paper web in a paper machine (Pramila 1986). Moreover, if the air field oscillates in a same phase as the structure, the translating membrane will behave dynamically as if its mass had increased by that of the vibrating air. With an axially moving narrow band this idealization leads to the following equation of motion of threadline (Pramila 1987)

$$\left(m + m_a\right)u_{,tt} + 2\,m\,v\,u_{,xt} + m\,v^2\,u_{,xx} - T\,u_{,xx} = f, \tag{2.16}$$

where the added mass per unit length m_a for a narrow band is

$$m_a = \frac{\rho_a \pi b^2}{4}\quad , \tag{2.17}$$

and ρ_a is the air density and b is the width of the translating band. A physical interpretation of the equation means that the air particles are assumed to move only in a plane perpendicular to the translation direction of the band. If particles are in motion in the translation direction, there should be additional mass terms in the Coriolis and centripetal inertia terms as well. The values of these additional terms will depend on the velocity of the air particles relative to the band. If the surrounding air moves in a longitudinal direction with the band, all the three added mass terms will be equal to above m_a. In the sense of an ideal fluid, the equation (2.16) is acceptable because an ideal fluid is non-viscous and does not "feel" the axial movement of the band. For the wider membranes, Pramila (1986) presents two equations for added mass,

$$m_a = \alpha\,\frac{\rho_a \pi L}{4} \qquad \& \qquad m_a = \beta\,\rho_a L, \tag{2.18}$$

where L is the length of a span and α and β are parameters depending on the relation b/L. At low axial velocities the latter equation one gives results which are closer to the experimental ones (Pramila 1987).

2.2.2. Fluid-structure interaction

If the above assumptions for incompressibility and the same phase vibration in the structure and air are not valid, the system should be treated as a fluid-structure interaction problem. The behaviour of the air can then be described with the acoustic wave equation for its pressure $p(x,y,z)$, known as Helmholz's equation:

$$\nabla^2 p = \frac{1}{c_a^2} \frac{\partial^2 p}{\partial t^2}, \tag{2.19}$$

where c_a is the speed of sound, t is time and ∇^2 is the Laplacian operator. Equation (2.19) can be derived from the Navier-Stokes equation of motion and a continuation equation by making the following assumptions (Laukkanen 1995):

- the fluid is compressible
- the fluid is non-viscous
- the flow is irrotational
- the average flow is not taken into account
- changes in the average fluid density and pressure in different areas of the fluid domain remain small.

The equation for interaction between a fluid and a structure can be obtained from the continuity requirement at an interface boundary. The normal directed displacement $u_n = \mathbf{u} \cdot \mathbf{n}$ of the structure must be identical to that of the fluid. Therefore, the equation of motion for air particles must be fulfilled at the interface boundary by normal displacements of the structure

$$\frac{\partial p}{\partial n} = -\rho_a \frac{\partial^2 u_n}{\partial t^2}, \tag{2.20}$$

where $\mathbf{n}$ represent the normal vector of the fluid-structure interface boundary outward from fluid domain. This equation can also be used at other boundaries. At a rigid boundary, the equation can be simplified to the form

$$\frac{\partial p}{\partial n} = 0. \tag{2.21}$$

If the dimensions of the fluid are large or infinite, the model in numerical analysis has to be cut off at some reasonable distance from the structure. Moreover, the reflection of pressure waves has to be prevented at the cutting boundaries to stop excitation from infinity. One way of doing this is to use radiation damping (Laukkanen 1995) and an other possibility is to let the boundary absorb the pressure wave, so that its energy vanishes. In order to dissipate the waves and their energy, an absorbing term has to be added to the boundary condition (2.20) (Rajaumar & Ali 1993)

$$\frac{\partial p}{\partial n} = -\rho_a \frac{\partial^2 u_n}{\partial t^2} + R \nabla \cdot \mathbf{v}, \tag{2.22}$$

where R is the acoustic resistance and $\nabla \cdot \mathbf{v}$ the velocity divergence. The term $R\nabla \cdot \mathbf{v}$ in equation (2.22) can be considered a force due to dissipating flow through an absorption layer at the boundary. Since $\partial p/\partial t$ is related to $\nabla \cdot \mathbf{v}$ via the conservation of mass equation for a compressible fluid

$$\nabla \cdot \mathbf{v} = -\frac{1}{\rho_a c_a^2} \frac{\partial p}{\partial t}, \tag{2.23}$$

the boundary absorption term can be written in the form

$$\frac{\partial p}{\partial n} = -\rho_a \frac{\partial^2 u_n}{\partial t^2} - \beta \left(\frac{1}{c_a} \frac{\partial p}{\partial t} \right), \tag{2.24}$$

where $\beta = R/\rho_a c_a$ is the nondimensional absorption coefficient of the sound absorbing material at the boundary. The valid range of coefficient β is from zero to unity. When $\beta = 0$, there is no energy loss at the boundary and the wall is rigid. For $\beta = 1$, all the energy incident on the boundary is lost, which represents a boundary left open, with no reflection of pressure waves (Rajaumar & Ali 1993).

2.3. Dynamic behaviour of a nonlinear structure

For small oscillations the response of a deformable structure can be adequately described by linear equations and boundary conditions, but as the amplitude of the oscillations increases, the influences of nonlinear effects grow, as also does the need to consider them. The sources of nonlinearities can be geometric, inertial, or material in nature. Typical geometric nonlinearity arises from midplane stretching of a thin structure coupled with transverse vibrations. This stretching leads to a nonlinear relationship between the strain and the displacement. Nonlinear inertial effects are caused by the presence of concentrated or distributed masses. Material nonlinearities occur whenever the stress is a nonlinear function of the strain (Nayfeh & Mook 1979).

Since exact solutions are not usually available, the problems are solved by approximated analysis using purely numerical techniques, analytical techniques or numerical-analytical techniques.

In general, the dynamic behaviour of a nonlinear structure is examined by considering its steady state response to a harmonic load. The response itself may be of an extremely complex structure. It may be either harmonic, subharmonic, or even chaotic (Thomson & Stewart 1986). In some cases a given harmonic load can lead to several different steady states, and which one is actually achieved will depend upon the initial conditions. Here we are mostly interested in harmonic steady states, some features of which will be discussed further below.

Typically, there are three types of resonance response to the harmonic case: softening springs, linear springs and hardening springs, see Fig. 8. The peak of the curve for the softening nonlinearity bends to the left, since the inherent frequency of the system decreases with increasing amplitude, while for hardening nonlinearity the curve bends to the right. Fig. 8 could represent equally well the response of a system with a single degree or that of a system with multiple degree of freedom near a particular resonant frequency.

The bending of the resonance response leads to multivalued amplitudes and hence to a jump phenomenon, as shown Fig. 9, which depicts a typical forced response curve for a damped nonlinear system, in which ω_n is the small amplitude linear natural frequency of the system and the 'backbone curve' gives the relationship between the free vibration frequency and the amplitude. If the frequency of excitation is slowly increased and the amplitude of excitation is held constant, the response amplitude will grow from point A and a jump will be observed at C to point E. If frequency is then reduced, another jump will be observed at F, following the well-known hysteresis. Between the frequencies ω_1 and ω_2 the response is non-unique and may lie either on BC or on EF, depending on the initial conditions.

Most common approximation methods for determining resonance response curves are perturbation methods, the harmonic balance method and time integration methods. Perturbation methods perform satisfactorily if the nonlinearities of the dynamic system are of a small order. The nonlinear terms are referred to as "perturbations" and are identified by means of a small parameter. The solution is commonly sought in the form of a power series on this parameter.

The harmonic balance method is a simple, systematic approach and is not restricted to weakly nonlinear problems. The technique is based on a Fourier series residual approximation of the nonlinear terms, converting the nonlinear differential equations of motion to nonlinear algebraic equations.

In time integration methods the response of the nonlinear system is calculated by integrating the equation of motion numerically until a steady state is obtained, at the time when the transient effects are damped. This method is easy to apply to different kinds of nonlinear system, but it is costly, especially in the case of lightly damped, stiff structures with a large number of degrees of freedom.

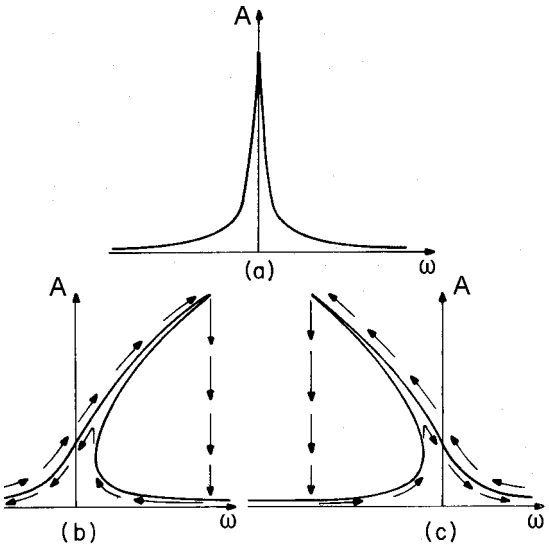

Fig. 8. Typical resonance response curves for harmonic response: a) a linear spring, b) a softening spring and c) a hardening spring (Nayfeh & Mook 1979).

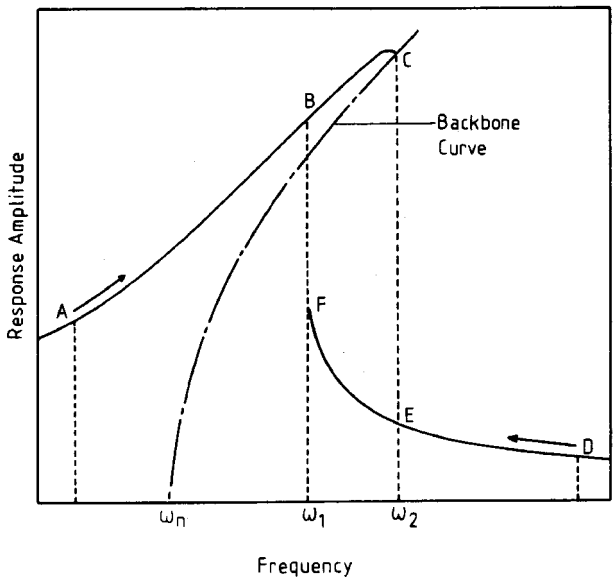

Fig. 9. Typical forced response curve for a nonlinear system (Thomson & Stewart 1986).

2.4. The physical model

The physical model to be considered here, as shown in Fig. 10, is a thin web passing over a free span between two supporting rolls at a prescribed velocity. During operation the membrane is stretched to a known tension, which comes from the support and drive mechanisms. Traditionally systems like this are considered in terms of a web of constant length between roll supports. This means that the supporting structures (cylinders) are idealized as “simple” line supports at fixed locations.

In some practical applications, however, (e.g. the web in a paper machine), it has been detected that when the band seats and unseats on the cylinder, the contact line moves along the roll depending on the position of the membrane. Thus, the free span length between the rolls is not a constant during vibration and the assumption of simple supports may be poor, at least in some cases.

In practice, we have two different possible approaches to formulating this kind of problem. First, we can consider a stretched translating membrane of a length that varies with time, or else we can move the boundaries so far along the support cylinders that the transverse displacements of the passing membrane are zero. The influence of contact between the membrane and the support cylinders must be included, however.

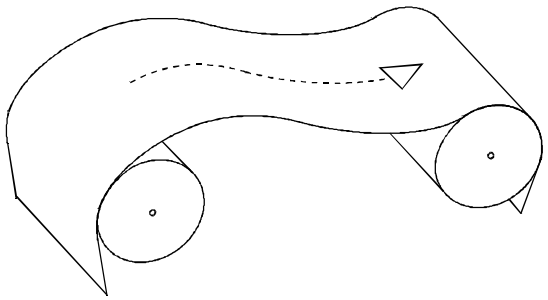

Fig. 10. The physical model.

2.4.1. A band of time varying length

We will restrict ourselves for the moment to examining only the vibrating part of the membrane passing over the span between the supporting cylinders (Fig. 11). An advantageous feature of this formulation is that it does not require consideration of the contact between the membrane and the supporting structures, whereas the disadvantage is that the mass of the system varies and therefore the particle flow through the boundaries has to be taken into account. The equations of motion are difficult to solve because the movement of the boundaries is coupled with the transverse motion of the membrane.

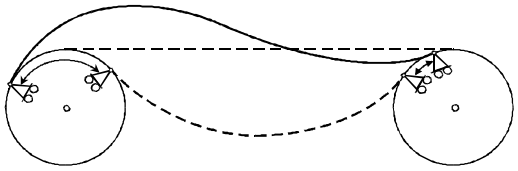

Fig. 11. A membrane of varying length.

Structures of varying length have been investigated in several theoretical considerations, including strings (Tagata 1983), beams (Zajaczkowski & Lipinski 1979, Zajaczkowski & Yamada 1980a), plates (Zajaczkowski & Yamada 1980b), axially moving strings (Popov 1986) and axially moving beams (Yue 1992). Popov considers a linear, longitudinally moving taut string, the length of which varies arbitrarily with time. This equation of motion is written in the form

$$\begin{aligned} &u_{,tt} + 2v\,u_{,xt} - \left(c^2 - v^2\right)u_{,xx} = 0\ , \quad x \in [0, L(t)] \\ &u(0,t) = u(L(t),t) = 0, \end{aligned} \tag{2.25}$$

where the right boundary moves according to the law $x = L(t)$ and c indicates the transverse wave propagation velocity of the string. Equation (2.25) for an axially moving string can be reduced by means of Galileo and Lorenz transformations to a wave equation for a string:

$$\begin{aligned} &u_{,t't'} - c^2 u_{,x'x'} = 0\ , \quad x' \in [0, \Lambda(t)] \\ &u(0,t') = u(\Lambda(t')) = 0, \end{aligned} \tag{2.26}$$

where t' and x' denote transformed time and space coordinates and

$$\Lambda(t') = L(t') - v\,t'. \tag{2.27}$$

The segment $[0, \Lambda(t)]$ may then be mapped to the segment $[0, l]$ by the function $f(x')$ and a one-dimensional wave equation for a string of constant length is obtained:

$$u_{,\tau\tau} - c^2 u_{,\xi\xi} = 0\ , \quad x \in [0, l], \tag{2.28}$$

where

$$\begin{aligned} \xi &= f\left(t' + \frac{x'}{c}\right) - f\left(t' - \frac{x'}{c}\right) \\ \tau &= \frac{1}{c}\left[f\left(t' + \frac{x'}{c}\right) + f\left(t' - \frac{x'}{c}\right)\right]. \end{aligned} \tag{2.29}$$

The difficulty with this method is finding out how to solve the function f from the functional equation

$$f\left(t' + \frac{\Lambda(t)}{c}\right) - f\left(t' - \frac{\Lambda(t)}{c}\right) = l. \tag{2.30}$$

Popov (1986) proposes solving an inverse problem instead of equation (2.30), though he cannot give any examples. For the case considering in this work, solving an inverse problem is particular demanding because of the coupling of boundary motion with transverse displacement of the membrane, so that the function f depends on these too.

Yue (1992), examining the influence of contact point movement on the dynamic behaviour of a belt/pulley system, introduced the concept of *a vibrating length L* for the actual free span length. The reasons for the variation in free length were explained as curving of the belt due to flexural stiffness, bending of the belt about the guiding pulley and movement in the contact points during vibration along the pulleys when the belt seats and unseats the pulley.

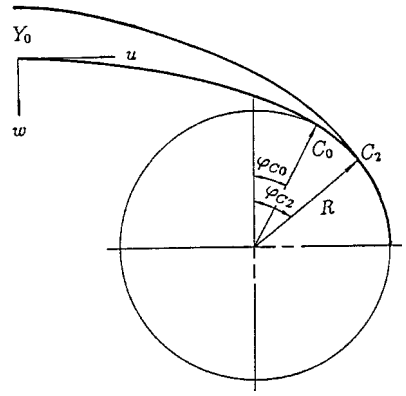

Fig. 12. Contact point motion (Yue 1992).

The initial shape of the free span and the initial location of the contact points were defined through the equilibrium equation for a beam. The position of the contact points for dynamic analysis was obtained using the following constraints:

1) the contacting pulley and belt must have the same transverse displacement value at the contact point x_c, and
2) the belt must have the same radius of curvature as the pulley at the contact point x_c.

The resulting equation of motion was solved numerically. According to the results presented by Yue's (1992), the contact point of the belt and pulley moves along the pulley depending on its pitch radius and the amplitude of the transverse vibration of the belt. Moreover, any increase in the vibration length L will increase the fundamental natural

frequency of the belt, which is against the linear theory.

2.4.2. A band with fixed boundaries

If we examine a structure with the fixed boundaries, the boundary points have to be selected on the support cylinders so that the transverse displacements of the passing membrane are zero (Fig. 13). The reason for this condition derives from the simplification of an open boundary application of Hamilton's principle to a normal closed system form (see page 39). The formulation of the equations of motion is now obvious, but solution of the equation is harder, due to the modelling of the contact between the support cylinders and the membrane. No analysis of this kind is known to have been performed to date for axially moving structures.

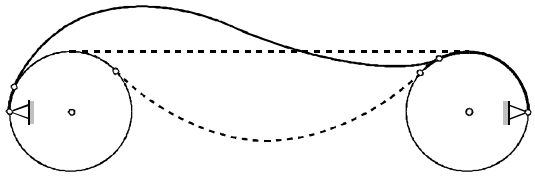

Fig. 13. A band with fixed boundaries.

3. Theoretical model of an axially moving membrane

Of the two possible formulation methods (section 2.4) we chose the constant length membrane model, because it allows a theoretical model for an axially moving membrane to be formulated as a general case involving only a few restrictions. A numerical formulation is also most probably easier to develop, because we can use an existing FEM program which includes a contact algorithm.

Since we are studying a thin, light membrane, the influence of the surrounding air is significant, and since we are examining the effects of boundary point movement, the displacements are large. Thus the theoretical model should include the fluid/membrane coupling and the nonlinear terms arising from large amplitude oscillations, variation in tension along the membrane and contact between the membrane and the rolls. Flexural stiffness can be neglected due to the assumption of a thin membrane, and deformations in the membrane can be described with the Lagrangian strain of a middle surface. The material behaviour of the membrane (paper) is not modelled in detail, because our interest is directed at the dynamic phenomena of an axially moving thin membrane. The material is therefore described with a hyperelastic model.

Since we wish to formulate the general boundary value problem of nonlinear continuum mechanics in a way oriented toward numerical methods, we will use an incremental description of the deformation process. The incremental equations for the membrane are developed through the analysis of prestressed elastic structures in the same way as outlined by Reismann & Pawlik (1977) for hyperelastic solids and applied by Luongo *et al.* (1984) to an elastic cable and Perkins & Mote (1987) to a travelling cable, taking account the remarks made in section 2.1.2. Membrane elasticity is included via a finite strain model and the membrane transport speed is included through a kinematical study, which with the convected coordinate practice allows the variation in transport motion to be considered as well. The equations of motion are developed using Hamilton's principle.

The nonlinear dynamic behaviour is examined by determining the response resulting from harmonic boundary excitation. This response is calculated by direct time integration of equations of motion for each excitation frequency until the steady state is obtained. The method requires a lot of computer time, but because of the contact with surrounding structures, other methods such as the harmonic balance and perturbation are most likely impossible.

3.1. An initially stressed axially moving membrane

Tensor notations will be used throughout the following formulation. The left superscript indicates in which configuration the quantity occurs and the left subscript shows the configuration with respect to which it is measured. For example, the Green-Lagrange strain ${}^{F}_{o}\gamma_{\alpha\beta}$ in state ${}^{F}\chi$ is measured with respect to the natural state ${}^{o}\chi$. If the quantity considered occurs in the same configuration where it is measured, the left subscript will be omitted and incremental quantities will be shown without the left superscript. The right Greek letter scripts are tensor indices reserved for surface quantities and have only the values 1, 2, while the Latin indices have the values 1, 2, 3. The summation convention for repeated indices applies unless otherwise indicated.

The equations for the axially moving membrane are developed based upon the following assumptions:

1. The membrane is assumed to be a smooth, continuous, differentiable surface. The thickness ${}^{I}h$ of the membrane in the initial state is small compared with the smallest radius of curvature.
2. The membrane is so thin that the flexural stiffness can be omitted.
3. Deformations of the membrane can be described by the Lagrangian strains of the middle surface.
4. The material flow is homogeneous.
5. The flow through the boundary takes place where the displacements perpendicular to the flow are fixed.
6. The membrane is hyperelastic.
7. An arbitrary prestress causes the initial deformation from the natural state to the initial state.

An elastic travelling membrane passing through two fixed boundaries is modelled as a two-dimensional continuum. Since the membrane is assumed to be hyperelastic, its constitution is completely characterized by the strain energy density function, and three configurations can be distinguished (Fig. 14).

(1) The natural configuration ${}^{o}\chi$ is a state in which all stress resultants $n^{\alpha\beta}$, strains $\gamma_{\alpha\beta}$ and the strain energy density function W^{*} vanish, this means also lack of transport motion.

(2) The initial configuration ${}^{I}\chi$ corresponds to an equilibrium state (steady state) in the membrane, and

(3) the final (current) configuration ${}^{F}\chi$ is the desired unknown state.

Because of the travelling motion of the membrane, neither Lagrangian (material) nor Eulerian (spatial) descriptions are used, but a “mixed” description is developed as discussed

in section 2.1.2. The coordinate system is defined using the natural configuration as a base membrane in which a net of coordinate curves θ^1 and θ^2 is drawn. These curves can be transferred to the initial and final configuration by imaging pieces of membrane cut off from between the fixed displacement supports. After the removal of stresses, these pieces are placed on the base piece ${}^{o}\chi$ for copying of the coordinate curves onto the sample points of the configuration. This assumption requires that a detached piece considered at an arbitrary moment must be a "clone" of the base piece ${}^{o}\chi$, and as a result we have a convected coordinate system attached to the sample points of the configurations. The tensor components will be presented by reference to this convected coordinate system for the middle surface of the membrane configuration.

The finite deformation of a membrane may be described by considering the path from the initial configuration ${}^{I}\chi$ with location ${}^{I}\mathbf{x}\left(\theta^{\alpha}\right)$ to the final configuration ${}^{F}\chi$ with location ${}^{F}\mathbf{x}\left(\theta^{\alpha},t\right)$. The difference between these locations,

$$\mathbf{u}\left(\theta^{\alpha},t\right) = {}^{F}\mathbf{x}\left(\theta^{\alpha},t\right) - {}^{I}\mathbf{x}\left(\theta^{\alpha}\right) , \tag{3.1}$$

represents the three-dimensional incremental motion of the membrane configuration (sample points) and is distinguished from the motion of a membrane particle that includes the transport motion. Since the results of any measurements performed on a prestressed body are obtained in terms of the initial coordinates, we will ultimately express all the results in terms of the initial configuration.

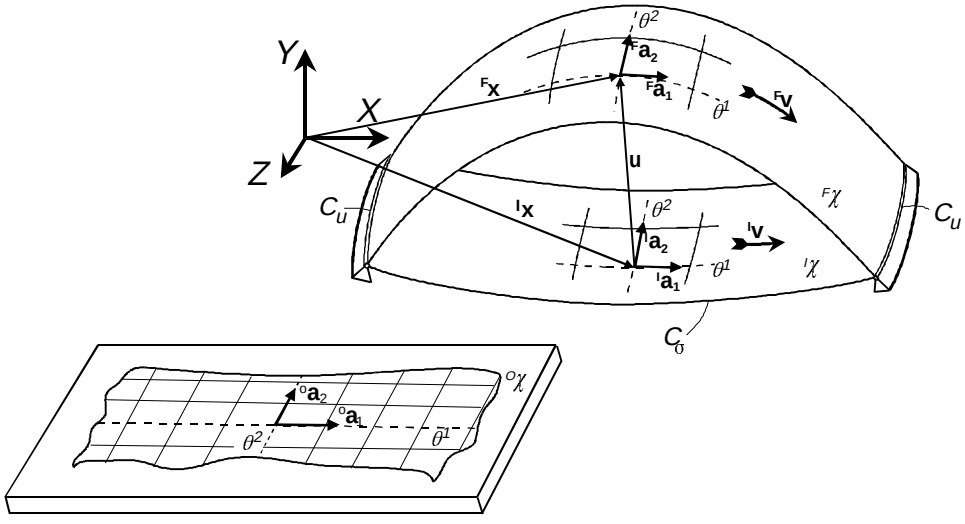

Fig. 14. The configurations of a membrane.

3.1.1. Incremental strain

The Lagrange strain tensor, Cauchy stress resultant tensor and constitutive relations are defined by the familiar relations (Green & Zerna 1968 and Niordson 1985)

$$ {}^{F}_{o}\gamma_{\alpha\beta} = \frac{1}{2}\left({}^{F}a_{\alpha\beta} - {}^{o}a_{\alpha\beta}\right) \tag{3.2} $$

$$ {}^{F}n^{\alpha\beta} = \frac{d\,{}^{o}A}{d\,{}^{F}A}\,{}^{F}_{o}\tilde{n}^{\alpha\beta} \tag{3.3} $$

$$ {}^{F}_{o}\tilde{n}^{\alpha\beta} = {}^{F}\left(\frac{\partial W^{*}}{\partial \gamma_{\alpha\beta}}\right) , \tag{3.4} $$

where ${}^{F}a_{\alpha\beta}$ and ${}^{o}a_{\alpha\beta}$ are covariant metric tensors of the surface in the final and natural configurations, ${}^{F}_{o}\tilde{n}^{\alpha\beta}$ is the second Piola-Kirchoff stress resultant tensor, ${}^{F}A$ and ${}^{o}A$ are the areas of the surface in the final and natural configurations and $W^{*} = W^{*}(\gamma_{\alpha\beta}, \theta^{\alpha})$ is the strain energy density function. The covariant base vectors of the surface at a material point $\boldsymbol{P}$ are given by

$$ {}^{F}\mathbf{a}_{\alpha} = \frac{\partial\,{}^{F}\mathbf{x}}{\partial \theta^{\alpha}} = {}^{F}\mathbf{x}_{,\alpha} \tag{3.5} $$

and the covariant metric tensor on the surface, $a_{\alpha\beta}$, is thus

$$ {}^{F}a_{\alpha\beta} = {}^{F}\mathbf{a}_{\alpha} \cdot {}^{F}\mathbf{a}_{\beta} = {}^{F}\mathbf{x}_{,\alpha} \cdot {}^{F}\mathbf{x}_{,\beta} . \tag{3.6} $$

Upon substitution of (3.1) into (3.6) we find that the total strain (3.2) can be separated into two parts

$$ {}^{F}_{o}\gamma_{\alpha\beta} = {}^{I}_{o}\gamma_{\alpha\beta} + {}_{I}\gamma_{\alpha\beta} , \tag{3.7} $$

that is, the initial strain

$$ {}^{I}_{o}\gamma_{\alpha\beta} = \frac{1}{2}\left({}^{I}a_{\alpha\beta} - {}^{o}a_{\alpha\beta}\right) \tag{3.8} $$

and the incremental strain

$$ {}_{I}\gamma_{\alpha\beta} = {}_{I}\varepsilon_{\alpha\beta} + {}_{I}\eta_{\alpha\beta} . \tag{3.9} $$

This is written as a sum of a linear part

$$ {}_I\varepsilon_{\alpha\beta} = \frac{1}{2}\left({}^I\mathbf{a}_\alpha \cdot \mathbf{u}_{,\beta} + \mathbf{u}_{,\alpha} \cdot {}^I\mathbf{a}_\beta \right) \tag{3.10} $$

and a nonlinear part

$$ {}_I\eta_{\alpha\beta} = \frac{1}{2}\left(\mathbf{u}_{,\alpha} \cdot \mathbf{u}_{,\beta} \right) . \tag{3.11} $$

3.1.2. Strain energy

In order to obtain an examination referring to the initial configuration, the strain energy density function will be developed in the form of Taylor's series in the neighbourhood of the initial state. We assume that the strain energy density function together with its partial derivatives up to and including the third order in strain exist and are continuous at ${}^I_o\gamma_{\alpha\beta}$ (the initial state). Based on the assumption of small incremental deformations, the series for the strain energy density is truncated after the quadratic terms. Therefore, the strain energy density is

$$ \begin{aligned} W^*\left({}^F_o\gamma_{\alpha\beta}\right) = W^*\left({}^I_o\gamma_{\alpha\beta}\right) + {}^I\left(\frac{\partial W^*}{\partial \gamma_{\alpha\beta}}\right)\left({}^F_o\gamma_{\alpha\beta} - {}^I_o\gamma_{\alpha\beta}\right) + \\ + \frac{1}{2}\,{}^I\left(\frac{\partial W^*}{\partial \gamma_{\alpha\beta}\,\partial \gamma_{\mu\lambda}}\right)\left({}^F_o\gamma_{\alpha\beta} - {}^I_o\gamma_{\alpha\beta}\right)\left({}^F_o\gamma_{\mu\lambda} - {}^I_o\gamma_{\mu\lambda}\right) + O^3\left({}_I\gamma_{\alpha\beta}\right) , \end{aligned} \tag{3.12} $$

or, using equations (3.3) and (3.7), it becomes

$$ {}^FW^* = {}^IW^* + {}^In^{\alpha\beta}\,{}_I\gamma_{\alpha\beta}\,\frac{d\,{}^IA}{d\,{}^oA} + \frac{1}{2}\,{}^IC^{\alpha\beta\mu\lambda}\,{}_I\gamma_{\alpha\beta}\,{}_I\gamma_{\mu\lambda}\,\frac{d\,{}^IA}{d\,{}^oA} + O^3\left({}_I\gamma_{\alpha\beta}\right) , \tag{3.13} $$

where

$$ {}^I_o\tilde{n}^{\alpha\beta} = {}^I\left(\frac{\partial W^*}{\partial \gamma_{\alpha\beta}}\right) \tag{3.14} $$

is the second Piola-Kirchoff stress resultant for the initial state,

$$ {}^In^{\alpha\beta} = \frac{d\,{}^oA}{d\,{}^IA}\,{}^I_o\tilde{n}^{\alpha\beta} \tag{3.15} $$

is the Cauchy stress resultant for the initial state,

$$ {}^{I}_{o}C^{\alpha\beta\mu\lambda} = {}^{I}\left(\frac{\partial W^{*}}{\partial \gamma_{\alpha\beta}\, \partial \gamma_{\mu\lambda}} \right) = {}^{I}_{o}C^{\mu\lambda\alpha\beta} = {}^{I}_{o}C^{\beta\alpha\mu\lambda} = {}^{I}_{o}C^{\alpha\beta\lambda\mu} \tag{3.16} $$

is an elasticity tensor in the initial state with respect to the natural configuration and

$$ {}^{I}C^{\alpha\beta\mu\lambda} = \frac{d\,{}^{o}A}{d\,{}^{I}A}\; {}^{I}_{o}C^{\alpha\beta\mu\lambda} \tag{3.17} $$

is an elasticity tensor at initial state.

The assumption of small deformations does not lead here to a linear theory as is the case for a hyperelastic solid in as discussed by Reismann & Pawlik (1977), since ${}_{I}\gamma_{\alpha\beta}$ is now a nonlinear function of the displacement gradient caused by the possibly large displacements.

The total strain energy of the membrane is obtained by integrating the strain energy density function over the area of the membrane

$$ {}^{F}U = \int_{{}^{o}A} {}^{F}W^{*}\; d\,{}^{o}A = {}^{I}U^{*} + \int_{{}^{I}A} {}^{I}n^{\alpha\beta}\; {}_{I}\varepsilon_{\alpha\beta}\; d\,{}^{I}A + U\ , \tag{3.18} $$

where

$$ {}^{I}U^{*} = \int_{{}^{o}A} {}^{I}W^{*}\; d\,{}^{o}A \tag{3.19} $$

is the strain energy associated with the initial deformation, and

$$ U = \int_{{}^{I}A} \left({}^{I}n^{\alpha\beta}\; {}_{I}\eta_{\alpha\beta} + \frac{1}{2}\, {}^{I}C^{\alpha\beta\mu\lambda}\; {}_{I}\gamma_{\alpha\beta}\; {}_{I}\gamma_{\mu\lambda} \right) d\,{}^{I}A \tag{3.20} $$

is the incremental strain energy.

3.1.3. Stress increment

The constitutive relation for incremental deformations is derived by substituting a quadratic approximation ${}^{F}W^{*}$, equation (3.13), into right hand side of the second Piola-Kirchoff stress resultant equation (3.4):

$$
\begin{aligned}
{}^{F}_{o}\tilde{n}^{\alpha\beta} &= {}^{F}\left(\frac{\partial W^{*}}{\partial \gamma_{\alpha\beta}}\right) = {}^{I}\left(\frac{\partial W^{*}}{\partial \gamma_{\alpha\beta}}\right) + {}^{I}\left(\frac{\partial W^{*}}{\partial \gamma_{\alpha\beta}\partial \gamma_{\mu\lambda}}\right)\left({}^{F}_{o}\gamma_{\mu\lambda} - {}^{I}_{o}\gamma_{\mu\lambda}\right) \\
&= {}^{I}_{o}\tilde{n}^{\alpha\beta} + {}^{I}_{o}C^{\alpha\beta\mu\lambda}\,{}_{I}\gamma_{\mu\lambda} \\
&= \frac{d^{I}A}{d^{o}A}\left({}_{I}n^{\alpha\beta} + {}^{I}C^{\alpha\beta\mu\lambda}\,{}_{I}\gamma_{\mu\lambda}\right)
\end{aligned}
\tag{3.21}
$$

Now, if we use a transformation of the stresses (3.3)

$$
{}^{F}n^{\alpha\beta} = \frac{d^{o}A}{d^{F}A}\,{}^{F}_{o}\tilde{n}^{\alpha\beta} = \frac{d^{I}A}{d^{F}A}\,{}^{F}_{I}\tilde{n}^{\alpha\beta} \tag{3.22}
$$

and the above equation (3.21), we can write the final Piola-Kirchoff stress resultant with respect to initial state:

$$
\begin{aligned}
{}^{F}_{I}\tilde{n}^{\alpha\beta} &= \frac{d^{o}A}{d^{I}A}\,{}^{F}_{o}\tilde{n}^{\alpha\beta} = {}_{I}n^{\alpha\beta} + {}^{I}C^{\alpha\beta\mu\lambda}\,{}_{I}\gamma_{\mu\lambda} \\
&= {}_{I}n^{\alpha\beta} + {}_{I}\tilde{n}^{\alpha\beta}
\end{aligned}
\tag{3.23}
$$

The incremental constitutive equation is therefore

$$
{}_{I}\tilde{n}^{\alpha\beta} = {}^{I}C^{\alpha\beta\mu\lambda}\,{}_{I}\gamma_{\mu\lambda} \ . \tag{3.24}
$$

3.1.4. Hamilton's principle

The equations of motion can be obtained using Hamilton's principle. However, this is formulated in its traditional form for a closed system, i.e. for a system containing the same particles throughout. In this consideration a "mixed" formulation is used, so that the motion of the system is due to a movement of the configuration and the transport movement of passing material particles. Thus the particles which fill the domain are changing all the time and the energy flux across the boundaries must be taken into account. By assuming a special case in which the boundaries are fixed both at the inlet and at the outlet, the fluxes in and out are equal and the net energy flux through the boundaries is zero. Therefore, as shown by Benjamin (1961), McIver (1973) and Niemi & Pramila (1987), Hamilton's principle takes in this case the familiar form

$$
\int_{t_1}^{t_2}\left(\delta\,{}^{F}T - \delta\,{}^{F}U\right)\,dt = -\int_{t_1}^{t_2}\delta\,{}^{F}W\,dt\ , \tag{3.25}
$$

where $\delta\,{}^{F}T$ and $\delta\,{}^{F}U$ denote the variation of total kinetic energy and potential energy for the current state and $\delta\,{}^{F}W$ denotes the work done by external forces as a result of the variation $\delta\mathbf{u}$.

3.1.5. Variation of kinetic energy

The kinetic energy of the membrane in the final state is given by

$$ {}^{F}T = \int_{{}^{F}A} {}^{F}\mathbf{w} \cdot {}^{F}\mathbf{w}\ {}^{F}\rho\ {}^{F}h\ d\,{}^{F}A\ , \tag{3.26} $$

where ${}^{F}\mathbf{w}$ represents the velocity of a membrane particle associated with ${}^{F}\chi$. The kinetic energy expression differs from that for a conventional system because of the "mixed" description of motion. The motion of a material particle consists of the movement of the configuration $\mathbf{x} = \mathbf{x}\left(\theta^{\alpha}, t\right)$ and the transport movement of the passing particles. The velocity of a material particle is therefore

$$ {}^{F}\mathbf{w} = {}^{F}\mathbf{x}_{,t} + {}^{F}\mathbf{v}\ . \tag{3.27} $$

The transport velocity vector $\mathbf{v}$ is not a constant parameter but changes with the deformation, even if we assume that the material flow is constant. The changes in transport velocity can be developed using same kind of kinematic study as in section 2.1.2, and is shown in Fig. 15. The motion of a material particle is followed a during short time step dt from the point ${}^{I}P$ in the equilibrium (steady) state ${}^{I}\chi$ and from the corresponding sample point ${}^{F}P$ in the final state. The displacement of the particle in the equilibrium state consists only of the transport motion, and therefore it is

$$ \mathrm{d}\,{}^{I}\mathbf{x} = {}^{I}\mathbf{v}\,\mathrm{d}t = {}^{I}v^{\alpha}\,{}^{I}\mathbf{a}_{\alpha}\,\mathrm{d}t\,. \tag{3.28} $$

Due to the geometry of the middle surface of the membrane, the displacement is also

$$ \mathrm{d}\,{}^{I}\mathbf{x} = {}^{I}\mathbf{a}_{\alpha}\,\mathrm{d}\theta^{\alpha}\,. \tag{3.29} $$

A material particle at the corresponding sample point ${}^{F}P$ in the final state ${}^{F}\chi$ moves according to ${}^{F}\mathbf{w}\,\mathrm{d}t$. The displacement of the sample point ${}^{I}P$, the point in the configuration where the particle in question is located at time t, is $\mathbf{u} = \mathbf{u}\left(\theta^{\alpha}, t\right)$, and the displacement of a configuration point Q where the particle is located at time $t + \mathrm{d}t$, is

$$ \begin{aligned} \mathbf{u}_{Q} &= \mathbf{u} + \mathrm{d}\,\mathbf{u} = \mathbf{u} + \mathbf{u}_{,\alpha}\,\mathrm{d}\theta^{\alpha} + \mathbf{u}_{,t}\,\mathrm{d}t \\ &= \mathbf{u} + \mathbf{u}_{,\alpha}\,{}^{I}v^{\alpha}\,\mathrm{d}t + \mathbf{u}_{,t}\,\mathrm{d}t\ . \end{aligned} \tag{3.30} $$

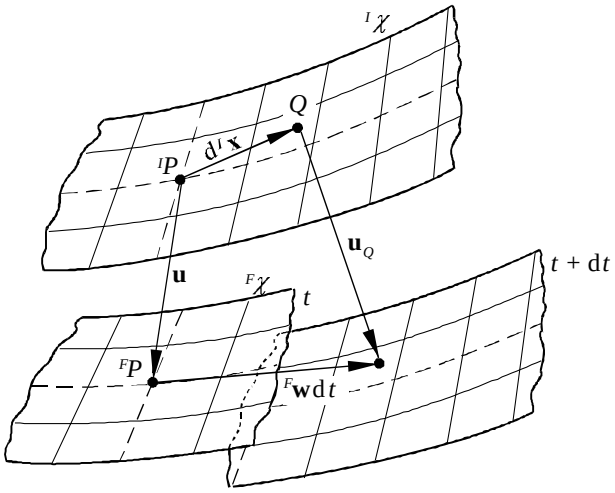

Fig. 15. Displacement of a point of the configuration and movement of a material particle.

The result was obtained by means of the chain rule and a scalar version of equation (3.28), $\mathrm{d}\theta^\alpha = v^\alpha\,\mathrm{d}t$. Finally, if we use the geometry of Fig. 15, develop a vector equation

$$\mathbf{u} + {}^F\mathbf{w}\,\mathrm{d}t = \mathrm{d}\,{}^I\mathbf{x} + \mathbf{u}_Q \tag{3.31}$$

and substitute equations (3.27), (3.28) and (3.30) into it, we obtain

$${}^F\mathbf{v} = {}^I\mathbf{v} + {}^Iv^\alpha\,\mathbf{u}_{,\alpha} = {}^Iv^\alpha\left({}^I\mathbf{a}_\alpha + \mathbf{u}_{,\alpha}\right) = {}^Iv^\alpha\,{}^F\mathbf{a}_\alpha\ . \tag{3.32}$$

The equation shows that the transport velocity is directed towards a tangential plane of the final configuration and that the convected components of the transport velocity vector are constants, i.e.

$${}^Fv^\alpha = {}^Iv^\alpha = v^\alpha\ . \tag{3.33}$$

The information on changes in the transport velocity vector on account of deformation is therefore included in the base vectors, as shown in the vector component representation

$${}^F\mathbf{v} = v^\alpha\,{}^F\mathbf{a}_\alpha\ . \tag{3.34}$$

As a consequence of equations (3.27) and (3.32), the velocity of a material particle can be written as

$${}^F\mathbf{w} = \mathbf{u}_{,t} + v^\alpha\left({}^I\mathbf{a}_\alpha + \mathbf{u}_{,\alpha}\right) \tag{3.35}$$

and its variation is

$$\delta\,{}^{F}\mathbf{w} \;=\; \delta\mathbf{u}_{,t} + v^{\alpha}\,\delta\mathbf{u}_{,\alpha}\;. \tag{3.36}$$

The laws of membrane mass conservation are a consequence of the assumption of a homogeneous flow. The configuration denoting the travelling membrane located between the fixed displacement supports has to retain a constant mass, or in other words

$$\int_{{}^{I}A} {}^{I}\rho\;\;{}^{I}h\;\,d\,{}^{I}A \;=\; \int_{{}^{F}A} {}^{F}\rho\;\;{}^{F}h\;\,d\,{}^{F}A\;. \tag{3.37}$$

Homogeneity also requires that every surface element in the configuration should keep its mass, so that

$${}^{I}\rho\;\;{}^{I}h\;\,d\,{}^{I}A \;=\; {}^{F}\rho\;\;{}^{F}h\;\,d\,{}^{F}A\;. \tag{3.38}$$

The variation of the kinetic energy of the membrane in the final state can now be written as

$$\begin{aligned}\delta\,{}^{F}T = \int_{{}^{I}A} \Big\{ &\Big(\mathbf{u}_{,t} + v^{\alpha}\left({}^{I}\mathbf{a}_{\alpha} + \mathbf{u}_{,\alpha}\right)\Big)\cdot(\delta\mathbf{u})_{,t} \;+ \\ &+ \Big(\mathbf{u}_{,t} + v^{\alpha}\left({}^{I}\mathbf{a}_{\alpha} + \mathbf{u}_{,\alpha}\right)\Big)\cdot v^{\beta}(\delta\mathbf{u})_{,\beta}\Big\}\;{}^{I}\rho\;\;{}^{I}h\;\,d\,{}^{I}A \;=\; \delta\,T\,.\end{aligned} \tag{3.39}$$

Integrating (3.39) by parts with respect to the middle surface and using Green's theorem to the developed terms, we obtain the following equation for the variation in kinetic energy

$$\begin{aligned}\delta T = \int_{{}^{I}A} \Big\{ &\Big(\mathbf{u}_{,t} + v^{\alpha}\left({}^{I}\mathbf{a}_{\alpha} + \mathbf{u}_{,\alpha}\right)\Big)\cdot(\delta\mathbf{u})_{,t} \;- \\ &- \Big[\sqrt{{}^{I}a}\,v^{\beta}\Big(\mathbf{u}_{,t} + v^{\alpha}\left({}^{I}\mathbf{a}_{\alpha} + \mathbf{u}_{,\alpha}\right)\Big)\Big]_{,\beta}\cdot\frac{\delta\mathbf{u}}{\sqrt{{}^{I}a}}\Big\}\;{}^{I}\rho\;\;{}^{I}h\;\,d\,{}^{I}A \;+ \\ &+ \oint_{{}^{I}C} v^{\beta}\,{}^{I}\hat{\mathfrak{v}}_{\beta}\Big(\mathbf{u}_{,t} + v^{\alpha}\left({}^{I}\mathbf{a}_{\alpha} + \mathbf{u}_{,\alpha}\right)\Big)\cdot\delta\mathbf{u}\;\,{}^{I}\rho\;\;{}^{I}h\;\,d\,{}^{I}s\;.\end{aligned} \tag{3.40}$$

where ${}^{I}\hat{\mathfrak{v}} = {}^{I}\hat{v}_{\alpha}\,{}^{I}\mathbf{a}^{\alpha}$ is a unit normal vector of the boundary of the membrane. The line integral in the above equation vanishes because there is no flow through the free boundary C_{σ}, and therefore $\mathbf{v}\cdot\hat{\mathfrak{v}} = 0$, while at the fixed boundary C_{u}, through which there is same flow, displacements are prevented, so that $\delta\mathbf{u} = 0$.

If we next integrate over the time interval t_1 to t_2 and integrate the first term by parts with respect to time, we obtain

$$\int_{t_1}^{t_2} \delta T \, dt = \int_{t_1}^{t_2} \Bigg(-\int_{{}^{I}A} \Big\{ \mathbf{u}_{,tt} + v^{\alpha} \mathbf{u}_{,t\alpha} + v^{\beta} \Big[\mathbf{u}_{,t} + v^{\alpha} \Big({}^{I}\mathbf{a}_{\alpha} + \mathbf{u}_{,\alpha} \Big) \Big]_{,\beta} \Big\} \cdot \delta \mathbf{u} \; {}^{I}\rho \; {}^{I}h \; d\,{}^{I}A + \int_{{}^{I}A} \frac{1}{\sqrt{{}^{I}a}} \Big(\sqrt{{}^{I}a}\, v^{\beta} \Big)_{,\beta} \Big[\mathbf{u}_{,t} + v^{\alpha} \Big({}^{I}\mathbf{a}_{\alpha} + \mathbf{u}_{,\alpha} \Big) \Big] \cdot \delta \mathbf{u} \; {}^{I}\rho \; {}^{I}h \; d\,{}^{I}A \Bigg) \, dt . \tag{3.41}$$

The substitution term of the integral vanishes because the variations $\delta\mathbf{u}(\theta^{\alpha},t_1) = \delta\mathbf{u}(\theta^{\alpha},t_2) = 0$. The second integral of the above equation can be transformed to a line integral using the divergence theorem

$$\int_{{}^{I}A} \Big(\nabla \cdot {}^{I}\mathbf{v} \Big) \Big({}^{F}\mathbf{w} \cdot \delta \mathbf{u} \Big) \; {}^{I}\rho \; {}^{I}h \; d\,{}^{I}A = \oint_{{}^{I}C} {}^{I}\rho \Big({}^{F}\mathbf{w} \cdot \delta \mathbf{u} \Big) \Big({}^{I}\mathbf{v} \cdot \hat{\mathfrak{v}} \Big) \, {}^{I}h \; d\,{}^{I}A \; . \tag{3.42}$$

The line integral may be thought of as virtual momentum transport across the open boundary C_u. Now because of the fixed displacements the variation $\delta\mathbf{u}$ is zero and the virtual momentum is zero, so that the eventual variation in kinetic energy is

$$\delta T = -\int_{{}^{I}A} \Big\{ \mathbf{u}_{,tt} + 2\, v^{\alpha} \mathbf{u}_{,t\alpha} + v^{\beta} \Big[v^{\alpha} \Big({}^{I}\mathbf{a}_{\alpha} + \mathbf{u}_{,\alpha} \Big) \Big]_{,\beta} \Big\} \cdot \delta \mathbf{u} \; {}^{I}\rho \; {}^{I}h \; d\,{}^{I}A \; . \tag{3.43}$$

The acceleration of a particle in a travelling membrane can be developed from the change in velocity as in the section 2.1.2. The process is shown in Appendix A. This results in the same form as the inertial terms obtained by means of Hamilton's principle in equation (3.43).

3.1.6. Variation of strain energy

The variation of strain energy is derived from the equation (3.18)

$$\delta\, {}^{F}U = \delta\, {}^{I}U^{*} + \delta\, {}^{I}U + \delta U \; , \tag{3.44}$$

where the variation of strain energy associated with the initial deformation

$$\delta\, {}^{I}U^{*} = 0 \; , \tag{3.45}$$

since ${}^{I}\chi$ is an equilibrium configuration. The variation of strain energy $\delta\, {}^{I}U$ in equation (3.44) is derived according Green & Zerna (1968):

$$
\begin{aligned}
\delta\, {}^{I}U &= \int_{{}^{I}A} {}^{I}n^{\alpha\beta}\, \delta\, {}_{I}\varepsilon_{\alpha\beta}\, d\, {}^{I}A \\
&= \int_{{}^{I}A} {}^{I}n^{\alpha\beta}\ {}^{I}\mathbf{a}_{\alpha} \cdot (\delta\mathbf{u})_{,\beta}\ d\, {}^{I}A \\
&= \int_{{}^{I}C_{\sigma}} {}^{I}n^{\alpha\beta}\ {}^{I}\mathbf{a}_{\alpha} \cdot \delta\mathbf{u}\ {}^{I}\vartheta_{\beta}\ d\, {}^{I}s - \int_{{}^{I}A} \left(\sqrt{{}^{I}a}\ {}^{I}n^{\alpha\beta}\ {}^{I}\mathbf{a}_{\alpha}\right)_{,\beta} \cdot \delta\mathbf{u}\, \frac{d\, {}^{I}A}{\sqrt{{}^{I}a}} \\
&= \int_{{}^{I}C_{\sigma}} {}^{I}\mathbf{n} \cdot \delta\mathbf{u}\ d\, {}^{I}s + \int_{{}^{I}A} \left({}^{I}\mathbf{p} + {}^{I}\rho\ {}^{I}h\ {}^{I}\mathbf{f}\right) \cdot \delta\mathbf{u}\ d\, {}^{I}A \quad ,
\end{aligned}
\tag{3.46}
$$

using Green's theorem to transform area to line integrals and then the equilibrium conditions of the initial configuration

$$
\begin{aligned}
&\left(\sqrt{{}^{I}a}\ {}^{I}n^{\alpha\beta}\ {}^{I}\mathbf{a}_{\alpha}\right)_{,\beta} + {}^{I}\mathbf{p} + {}^{I}\rho\ {}^{I}h\ {}^{I}\mathbf{f} = 0 \qquad && \text{on } {}^{I}A \\
&{}^{I}\mathbf{n} = {}^{I}\vartheta_{\alpha}\ {}^{I}n^{\alpha\beta}\ {}^{I}\mathbf{a}_{\beta} && \text{on } {}^{I}C \ ,
\end{aligned}
\tag{3.47}
$$

where ${}^{I}\mathbf{p}$ is surface traction per unit initial area, ${}^{I}\mathbf{f}$ is body force per unit initial volume and ${}^{I}\mathbf{n}$ is edge force per unit initial length. The boundary curve of the membrane ${}^{I}C$ is assumed to be closed and divided into a free boundary ${}^{I}C_{\sigma}$ and a fixed displacement boundary ${}^{I}C_{u}$.

The variation of incremental strain energy δU in (3.44) is derived using Green's theorem, yielding

$$
\begin{aligned}
\delta U &= \int_{{}^{I}A} \left\{ {}^{I}n^{\alpha\beta}\, \delta\, {}_{I}\eta_{\alpha\beta} + {}^{I}C^{\alpha\beta\mu\lambda}\ {}_{I}\gamma_{\mu\lambda}\, \delta\, {}_{I}\gamma_{\alpha\beta} \right\} d\, {}^{I}A \\
&= \int_{{}^{I}A} \left\{ {}^{I}n^{\alpha\beta}\ \mathbf{u}_{,\alpha} + {}_{I}\tilde{n}^{\alpha\beta} \left({}^{I}\mathbf{a}_{\alpha} + \mathbf{u}_{,\alpha}\right) \right\} \cdot (\delta\mathbf{u})_{,\beta}\, d\, {}^{I}A \\
&= \int_{{}^{I}C_{\sigma}} \left\{ {}^{I}n^{\alpha\beta}\, \mathbf{u}_{,\alpha} + {}_{I}\tilde{n}^{\alpha\beta} \left({}^{I}\mathbf{a}_{\alpha} + \mathbf{u}_{,\alpha}\right) \right\} \cdot \delta\mathbf{u}\ \vartheta_{\beta}\, d\, {}^{I}s \\
&\qquad - \int_{{}^{I}A} \left\{ \sqrt{{}^{I}a}\ {}^{I}n^{\alpha\beta}\, \mathbf{u}_{,\alpha} + \sqrt{{}^{I}a}\ {}_{I}\tilde{n}^{\alpha\beta} \left({}^{I}\mathbf{a}_{\alpha} + \mathbf{u}_{,\alpha}\right) \right\}_{,\beta} \cdot \delta\mathbf{u}\, \frac{d\, {}^{I}A}{\sqrt{{}^{I}a}} \, .
\end{aligned}
\tag{3.48}
$$

3.1.7. Virtual external work

The external forces currently acting on the membrane consist of a surface traction ${}^{F}\mathbf{p}$ per unit current area, an edge force ${}^{F}\mathbf{n}$ per unit current boundary and a body force ${}^{F}\mathbf{f}$ per unit current volume. The work done by these forces due to the virtual displacement $\delta\mathbf{u}$ is

$$\delta\, {}^{F}W = \int_{{}^{F}C_{\sigma}} {}^{F}\mathbf{n}\cdot\delta\mathbf{u}\; d\,{}^{F}s + \int_{{}^{F}A} \left({}^{F}\mathbf{p}\cdot\delta\mathbf{u} + {}^{F}\rho\; {}^{F}h\; {}^{F}\mathbf{f}\cdot\delta\mathbf{u}\right) d\,{}^{F}A \quad . \tag{3.49}$$

If we use conservation of mass (3.38) and similar transformation to that in equation (3.3) to transform the integrals in equation (3.49) from the current configuration ${}^{F}\chi$ to the initial configuration ${}^{I}\chi$, this yields

$$\begin{aligned} \delta\, {}^{F}W &= \int_{{}^{I}C_{\sigma}} {}^{F}\mathbf{n}\cdot\delta\mathbf{u}\; \frac{d\,{}^{F}s}{d\,{}^{I}s}\, d\,{}^{I}s + \int_{{}^{I}A} {}^{F}\mathbf{p}\cdot\delta\mathbf{u}\; \frac{d\,{}^{F}A}{d\,{}^{I}A}\, d\,{}^{I}A + \int_{{}^{I}A} {}^{I}\rho\; {}^{I}h\; {}^{F}\mathbf{f}\cdot\delta\mathbf{u}\; d\,{}^{I}A \\ &= \int_{{}^{I}C_{\sigma}} {}^{F}_{I}\mathbf{n}\cdot\delta\mathbf{u}\; d\,{}^{I}s + \int_{{}^{I}A} \left({}^{F}_{I}\mathbf{p}\cdot\delta\mathbf{u} + {}^{I}\rho\; {}^{I}h\; {}^{F}\mathbf{f}\cdot\delta\mathbf{u}\right) d\,{}^{I}A \quad , \end{aligned} \tag{3.50}$$

where we have introduced the notations ${}^{F}_{I}\mathbf{n}$ and ${}^{F}_{I}\mathbf{p}$ to be present the values of the final forces per unit initial area and initial arc length, i.e.

$${}^{F}_{I}\mathbf{n} = {}^{F}\mathbf{n}\; \frac{d\,{}^{F}s}{d\,{}^{I}s}, \qquad {}^{F}_{I}\mathbf{p} = {}^{F}\mathbf{p}\; \frac{d\,{}^{F}A}{d\,{}^{I}A} \quad . \tag{3.51}$$

Moreover, we define the incremental edge force ${}_{I}\mathbf{n}$, the incremental surface traction ${}_{I}\mathbf{p}$ and the incremental body forces ${}_{I}\mathbf{f}$, by the relations

$${}_{I}\mathbf{n} = {}^{F}_{I}\mathbf{n} - {}^{I}\mathbf{n}, \qquad {}_{I}\mathbf{p} = {}^{F}_{I}\mathbf{p} - {}^{I}\mathbf{p}, \qquad {}_{I}\mathbf{f} = {}^{F}\mathbf{f} - {}^{I}\mathbf{f} \quad . \tag{3.52}$$

Finally, by substituting equation (3.52) into (3.50) we obtain the work done by external current forces due to the virtual displacement, in the form

$$\delta\, {}^{F}W = \delta\, {}^{I}W + \delta W \quad , \tag{3.53}$$

where

$$\delta\, {}^{I}W = \int_{{}^{I}C_{\sigma}} {}^{I}\mathbf{n}\cdot\delta\mathbf{u}\; d\,{}^{I}s + \int_{{}^{I}A} \left({}^{I}\mathbf{p}\cdot\delta\mathbf{u} + {}^{I}\rho\; {}^{I}h\; {}^{I}\mathbf{f}\cdot\delta\mathbf{u}\right) d\,{}^{I}A \tag{3.54}$$

and

$$\delta W = \int_{{}^{I}C_\sigma} {}_{I}\mathbf{n}\cdot\delta\mathbf{u}\; d\,{}^{I}s + \int_{{}^{I}A} \left({}_{I}\mathbf{p}\cdot\delta\mathbf{u} + {}^{I}\rho\,{}^{I}h\,{}_{I}\mathbf{f}\cdot\delta\mathbf{u}\right) d\,{}^{I}A \ . \tag{3.55}$$

3.1.8. Equation of motion

The variational principle governing the incremental motion may be now obtained by substituting (3.39), (3.44) and (3.53) into (3.25). With the aid of (3.46) and (3.54), this results in the variational equation

$$\int_{t_1}^{t_2} \left(\delta T - \delta U + \delta W\right) dt = 0 \ . \tag{3.56}$$

The use of (3.43), (3.48) and (3.55) in (3.56) yield the equations of motion and associated boundary conditions in terms of incremental displacements

$$\begin{aligned} &\frac{1}{\sqrt{{}^{I}a}}\left[\sqrt{{}^{I}a}\;{}^{I}n^{\alpha\beta}\mathbf{u}_{,\alpha} + \sqrt{{}^{I}a}\;{}_{I}\tilde{n}^{\alpha\beta}\left({}^{I}\mathbf{a}_{\alpha} + \mathbf{u}_{,\alpha}\right)\right]_{,\beta} + {}_{I}\mathbf{p} + {}^{I}\rho\,{}^{I}h\,{}_{I}\mathbf{f} = \\ &= {}^{I}\rho\,{}^{I}h\left\{\mathbf{u}_{,tt} + 2\,v^{\alpha}\mathbf{u}_{,t\alpha} + v^{\beta}\left[v^{\alpha}\left({}^{I}\mathbf{a}_{\alpha} + \mathbf{u}_{,\alpha}\right)\right]_{,\beta}\right\} \end{aligned} \qquad \text{on } {}^{I}A \tag{3.57}$$

$$\mathbf{u} = \mathbf{U}\left(\theta^{\alpha}\right) \qquad \text{on } {}^{I}C_u \tag{3.58}$$

$$\left[{}^{I}n^{\alpha\beta}\mathbf{u}_{,\alpha} + {}_{I}\tilde{n}^{\alpha\beta}\left({}^{I}\mathbf{a}_{\alpha} + \mathbf{u}_{,\alpha}\right)\right]{}^{I}\vartheta_{\beta} = {}_{I}\mathbf{n} \qquad \text{on } {}^{I}C_\sigma \ . \tag{3.59}$$

The equation of equilibrium can be extracted from equation of (3.57) according to Perkins & Mote (1987) by setting all the time derivatives, **u** and incremental external forces to zero and it becomes

$$\frac{1}{\sqrt{{}^{I}a}}\left(\sqrt{{}^{I}a}\;{}_{I}\tilde{n}^{\alpha\beta}\,{}^{I}\mathbf{a}_{\alpha}\right)_{,\beta} = {}^{I}\rho\,{}^{I}h\;v^{\beta}\left(v^{\alpha}\,{}^{I}\mathbf{a}_{\alpha}\right)_{,\beta} \tag{3.60}$$

3.2. A thin web passing over a span between two finite cylinders

A common application for an axially moving membrane is a web moving over a span between two finite rollers. Examples of this kind can be found in paper machines, offset printing presses and magnetic tape devices. The following additional assumptions are made:

1. The curvature in a cross direction is zero in the initial state.
2. Another main direction in the initial state is the same as the direction of axial movement.
3. The body forces are zero.

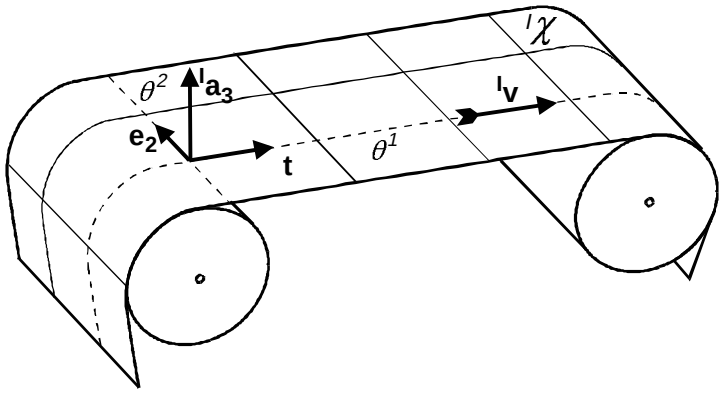

Fig. 16. Initial configuration of an axially moving membrane system with supporting cylinders.

In view of these assumptions, the geometry of the initial configuration is a simple cylindrical shell (Green & Zerna 1968). If we choose the convected coordinates as shown in Fig. 16, the convected base vectors of the middle surface in the initial state form a unit normal right-handed base

$$ {}^I\mathbf{a}_1 = \frac{\partial\, {}^I\mathbf{x}}{\partial \theta^1} = \mathbf{t}, \qquad {}^I\mathbf{a}_2 = \mathbf{e}_2, \qquad {}^I\mathbf{a}_3 = -\frac{1}{\kappa}\frac{\partial\, \mathbf{t}}{\partial \theta^1}, \tag{3.61} $$

where ${}^I\mathbf{a}_1$ is a unit tangent vector in a direction of axial movement denoted with $\mathbf{t}$, ${}^I\mathbf{a}_2$ is a constant unit vector denoted by $\mathbf{e}_2$, ${}^I\mathbf{a}_3$ is the unit normal to the middle surface and κ is the curvature at a point on the coordinate curve θ^1.

The derivatives of the base vectors in the initial state are

$$
\begin{aligned}
{}^I\mathbf{a}_{1,1} &= -\kappa\, {}^I\mathbf{a}_3 \\
{}^I\mathbf{a}_{1,2} &= {}^I\mathbf{a}_{2,1} = {}^I\mathbf{a}_{2,2} = 0,
\end{aligned}
\tag{3.62}
$$

and the determinant of the metric tensor in the initial state is

$$
{}^Ia = |{}^Ia_{\alpha\beta}| = 1 \ . \tag{3.63}
$$

Using the above assumptions, the equations of equilibrium (3.47) reduce to

$$
\begin{aligned}
{}^In^{11}{}_{,1} + {}^In^{12}{}_{,2} &= 0 \\
{}^In^{21}{}_{,1} + {}^In^{22}{}_{,2} &= 0 \\
\kappa\, {}^In^{11} - {}^Ip &= 0 \ .
\end{aligned}
\tag{3.64}
$$

It should also be noted that the magnitude of the transport velocity vector is constant over the initial state, so that the divergence $\nabla \cdot {}^I\mathbf{v} = v_{,\alpha}$ is zero. The equations of motion (3.57) then become

$$
\begin{aligned}
{}^In^{\alpha\beta}\mathbf{u}_{,\alpha\beta} + \left[{}_I\tilde{n}^{\alpha\beta}\left({}^I\mathbf{a}_\alpha + \mathbf{u}_{,\alpha}\right)\right]_{,\beta} + {}_I\mathbf{p} = \\
= {}^I\rho\, {}^Ih\left\{\mathbf{u}_{,tt} + 2v\,\mathbf{u}_{,1t} + v^2\left(\kappa\, {}^I\mathbf{a}_3 + \mathbf{u}_{,11}\right)\right\} \qquad \text{on } {}^IA
\end{aligned}
\tag{3.65}
$$

and the boundary conditions are

$$
\mathbf{u} = \mathbf{U}\left(\theta^\alpha\right) \qquad \text{on } {}^IC_u \tag{3.66}
$$

$$
\left[{}^In^{\alpha\beta}\,\mathbf{u}_{,\alpha} + {}_I\tilde{n}^{\alpha\beta}\left({}^I\mathbf{a}_\alpha + \mathbf{u}_{,\alpha}\right)\right]{}^I\hat{v}_\beta = 0 \qquad \text{on } {}^IC_\sigma \ . \tag{3.67}
$$

3.3. An initially plane axially moving web between simple supports

Systems with supporting cylinders are traditionally considered without the effect of the finite diameter of the roll supports and are idealized as 'simple' supports along fixed lines (see. Fig. 17). The initial state is now a plane configuration and the convected base vectors in the initial state form a constant, unit normal, right-handed base

$$
{}^I\mathbf{a}_1 = \mathbf{e}_1, \qquad {}^I\mathbf{a}_2 = \mathbf{e}_2, \qquad {}^I\mathbf{a}_3 = \mathbf{e}_3 \ . \tag{3.68}
$$

The derivatives of the base vectors in the initial state vanish, because they are constant over

the membrane. Using the above assumptions, the equations of equilibrium (3.64) become

$$\begin{aligned} {}^{I}n^{11}{}_{,1} + {}^{I}n^{12}{}_{,2} &= 0 \\ {}^{I}n^{21}{}_{,1} + {}^{I}n^{22}{}_{,2} &= 0 \ , \end{aligned} \tag{3.69}$$

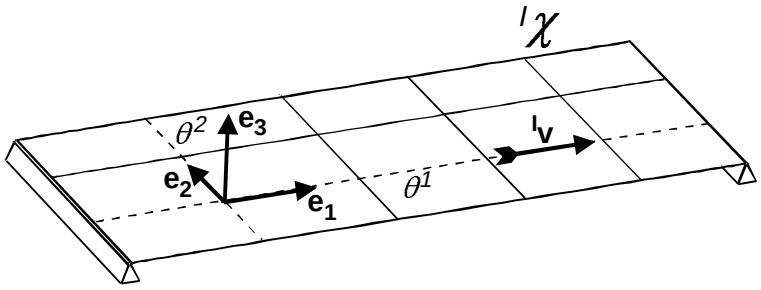

Fig. 17. Initial configuration of an axially moving plane membrane system.

the equations of motion (3.65) reduce to

$$\begin{aligned} \left({}^{I}n^{\alpha\beta} + {}_{I}\tilde{n}^{\alpha\beta}\right)\mathbf{u}_{,\alpha\beta} + {}_{I}\tilde{n}^{\alpha\beta}{}_{,\beta}\left({}^{I}\mathbf{a}_{\alpha} + \mathbf{u}_{,\alpha}\right) + {}_{I}\mathbf{p} = \\ = {}^{I}\rho\ {}^{I}h\left(\mathbf{u}_{,tt} + 2v\,\mathbf{u}_{,1t} + v^2\mathbf{u}_{,11}\right) \end{aligned} \quad \text{on } {}^{I}A \tag{3.70}$$

and the boundary conditions are

$$\mathbf{u} = \mathbf{U}\left(\theta^{\alpha}\right) \quad \text{on } {}^{I}C_{u} \tag{3.71}$$

$$\left[{}^{I}n^{\alpha\beta}\,\mathbf{u}_{,\alpha} + {}_{I}\tilde{n}^{\alpha\beta}\left({}^{I}\mathbf{a}_{\alpha} + \mathbf{u}_{,\alpha}\right)\right]{}^{I}\vartheta_{\beta} = 0 \quad \text{on } {}^{I}C_{\sigma} \ . \tag{3.72}$$

If we assume that the in plane displacements are small and can be ignored we obtain the equation of motion developed by Niemi & Pramila (1987), i.e.

$${}^{I}\rho\ {}^{I}h\left(u_{,tt} + 2v\,u_{,1t} + v^2u_{,11}\right) - \left({}^{I}n^{\alpha\beta} + {}_{I}\tilde{n}^{\alpha\beta}\right)u_{,\alpha\beta} + {}_{I}p = 0 \quad \text{on } {}^{I}A \ , \tag{3.73}$$

where transverse displacement is denoted by u and transverse incremental traction by ${}_{I}p$. This equation is obtained by noting that the stress resultants in the final state,

$${}^{F}n^{\alpha\beta} = \frac{d\,{}^{I}A}{d\,{}^{F}A}\left({}^{I}n^{\alpha\beta} + {}_{I}\tilde{n}^{\alpha\beta}\right) , \tag{3.74}$$

also fulfil the equilibrium equations (3.69).

4. Numerical consideration

The closed form solution of the incremental equations of motion (3.57) is very difficult or even impossible to calculate directly, since they are nonlinear in their displacement increments and base vectors, and therefore finite element method (FEM) will be used. For an effective numerical treatment of problem involving large displacements and large deformation, we use the incremental formulation (Kleiber 1989, Bathe 1982). There are two approaches to this formulation available:

1) total Lagrangian (TL) description in which the static and kinematic quantities refer to the initial configuration, and

2) updated Lagrangian (UL) description in which the static and kinematic quantities refer to the last calculated (current) configuration.

These two formulations are equivalent in a theoretical sense, and the motive for selecting one rather than the other is normally convenience, a reference configuration used in the constitutive law or greater numerical efficiency in a particular problem. Since we are using tensorial components of a convective coordinate system, these two types of formulation can be combined (Noguchi & Hisada 1995). The only difference is seen in the transformation of the constitutive tensorial components. We use the updated Lagrangian method, and hence the deformation of the membrane can be described by considering its path from an unknown undeformed configuration ${}^{o}\chi$ through the known initial configuration ${}^{I}\chi$ to the current deformed configuration ${}^{t}\chi$ and finally to a neighbouring unknown configuration, ${}^{t+\Delta t}\chi$, as illustrated in Fig. 18.

4.1. Equations for a discrete membrane

The governing equation of incremental motion for numerical development is derived by applying Hamilton's principle equation (3.25), as in chapter 3. The dynamic equilibrium of the membrane structure is evaluated at the discrete time points $0, \Delta t, 2\Delta t, 3\Delta t, \ldots$ from the initial state ${}^{I}\chi$ at time 0 with time steps of Δt. We assume that the solutions for the

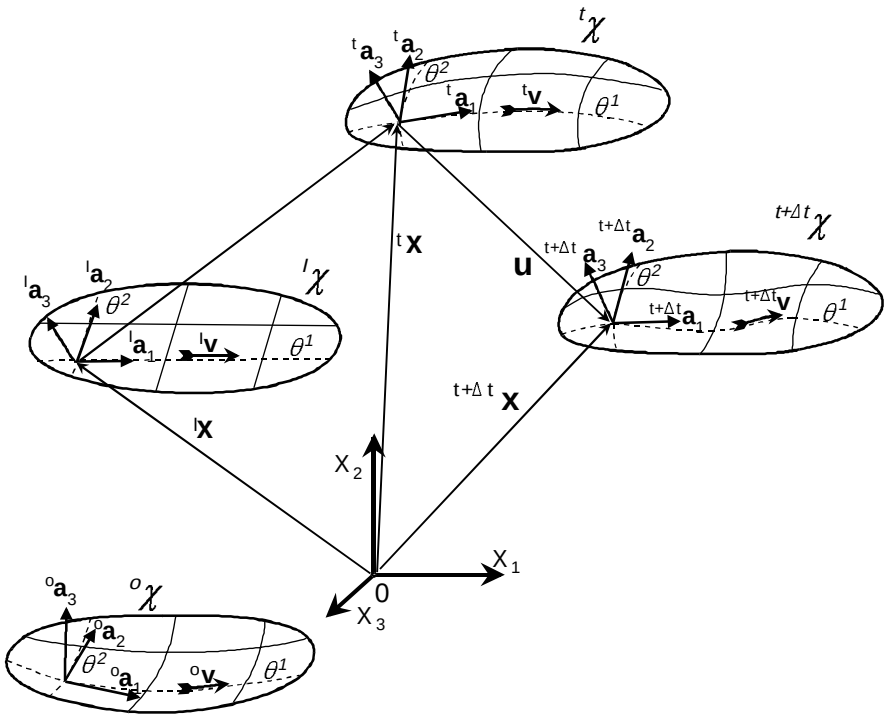

Fig. 18. Configurations in the path of deformation for FE analysis of initially stressed axially moving membrane.

kinematic and kinetic variables for all time steps from *0* to time *t* have been obtained, and then seek a solution for the next required equilibrium position, at time $t+\Delta t$. We denote the last known configuration, the reference configuration as ${}^{t}\chi$ and the new, unknown configuration as ${}^{t+\Delta t}\chi$.

Equations of motion are now obtained by marking the initial configuration ${}^{I}\chi$ as a current state at time *t* and the final configuration ${}^{F}\chi$ as an unknown state at time $t+\Delta t$ in Hamilton's principle (3.25). The equations of motion are now

$$
\begin{aligned}
-\int_{{}^{I}A} \left\{ \left[{}^{t+\Delta t}\mathbf{u}_{,t} + v^{\alpha} \left({}^{t}\mathbf{a}_{\alpha} + \mathbf{u}_{,\alpha} \right) \right] \cdot \delta \mathbf{u}_{,t} + \left[{}^{t+\Delta t}\mathbf{u}_{,t} + v^{\alpha} \left({}^{t}\mathbf{a}_{\alpha} + \mathbf{u}_{,\alpha} \right) \right] \cdot v^{\beta} \, \delta(\mathbf{u})_{,\beta} \right\} {}^{I}\rho \; {}^{I}h \; d\,{}^{I}A \; + \\
+ \int_{{}^{t}A} {}^{t}C^{\alpha\beta\mu\lambda} \, {}_{t}\gamma_{\mu\lambda} \; \delta_{t}\gamma_{\alpha\beta} \; d\,{}^{t}A \; + \int_{{}^{t}A} {}^{t}n^{\alpha\beta} \, \delta_{t}\eta_{\alpha\beta} \; d\,{}^{t}A \; = \; \delta^{\,t+\Delta t}W \; - \int_{{}^{t}A} {}^{t}n^{\alpha\beta} \, \delta_{t}\varepsilon_{\alpha\beta} \; d\,{}^{t}A \; ,
\end{aligned}
\tag{4.1}
$$

where ${}^{t}A$ denotes the area of the middle surface in the configuration ${}^{t}\chi$ and $\delta^{\,t+\Delta t}W$ is the external virtual work. The small displacement occurring during the time step Δt, a

displacement increment, is expressed by the subtraction

$$\mathbf{u} = {}^{t+\Delta t}\mathbf{x} - {}^{t}\mathbf{x}\ , \tag{4.2}$$

and the total displacement measured from the initial configuration ${}^{I}\chi$ at time *0* to the final configuration is

$${}^{t+\Delta t}\mathbf{u} = {}^{t+\Delta t}\mathbf{x} - {}^{I}\mathbf{x}. \tag{4.3}$$

The nonlinear term in the equation is linearized with the following assumption

$$\gamma_{\mu\lambda}\ \delta\gamma_{\alpha\beta} = \left(\varepsilon_{\mu\lambda} + \eta_{\mu\lambda}\right)\delta\left(\varepsilon_{\alpha\beta} + \eta_{\alpha\beta}\right) \approx \varepsilon_{\mu\lambda}\,\delta\varepsilon_{\alpha\beta}. \tag{4.4}$$

Moreover, we integrate the first term (variation of kinetic energy) by parts with respect to time and note that the variation of incremental strain is $\delta_t\gamma_{\alpha\beta} = \delta_t\varepsilon_{\alpha\beta} + \delta_t\eta_{\alpha\beta} = \left({}^{t}\mathbf{a}_{\alpha} + \mathbf{u}_{,\alpha}\right)\cdot\delta\mathbf{u}_{,\beta}$. The above notations result in

$$\begin{aligned}
&\int_{{}^{I}A}\left\{\left({}^{t+\Delta t}\mathbf{u}_{,tt} + v^{\alpha}\ {}^{t+\Delta t}\mathbf{u}_{,t\alpha}\right)\cdot\delta\mathbf{u} - v^{\beta}\ {}^{t+\Delta t}\mathbf{u}_{,t}\cdot\delta\mathbf{u}_{,\beta} - v^{\alpha}v^{\beta}\,\delta_t\eta_{\alpha\beta}\right\}\ {}^{I}\rho\ {}^{I}h\ d\,{}^{I}A + \\
&\quad + \int_{{}^{t}A} {}^{t}C^{\alpha\beta\mu\lambda}\ {}_{t}\varepsilon_{\mu\lambda}\ \delta_t\varepsilon_{\alpha\beta} + \int_{{}^{t}A} {}^{t}n^{\alpha\beta}\ \delta_t\eta_{\alpha\beta}\ d\,{}^{t}A = \\
&\qquad = {}^{t+\Delta t}W - \int_{{}^{t}A} {}^{t}n^{\alpha\beta}\,\delta_t\varepsilon_{\alpha\beta}\ d\,{}^{t}A + \int_{{}^{I}A} v^{\alpha}v^{\beta}\,\delta_t\varepsilon_{\alpha\beta}\ {}^{I}\rho\ {}^{I}h\ d\,{}^{I}A.
\end{aligned} \tag{4.5}$$

The equations shown in (4.5) are linear equations in the incremental displacement and are used to derive the governing finite element equations.

The membrane is subdivided into two-dimensional elements and the configuration and its movement is approximated by isoparametric interpolation, e.g. with the same shape functions N^A. The convected coordinates are chosen as the normal coordinates of the elements. This will eliminate the need for coordinate transformations, as the spatial derivatives with respect to the natural coordinates can be used directly in the formulation (Noguchi & Hisada 1995). The coordinate systems and the 12 degrees of freedom element used are shown in Fig. 19.

A point *P* on the middle surface of the membrane can be located with respect to the local convected coordinate system θ^{α}. The global coordinates, ${}^{t}x^{I}$, and global displacement components ${}^{t}u^{I}$, of *P* are given by

$${}^{t}x^{i} = N^{A}\ {}^{t}x_{A}^{i} \tag{4.6}$$

$${}^{t}u^{i} = N^{A}\ {}^{t}u_{A}^{i}\ , \tag{4.7}$$

where ${}^t x_A^i$ are the nodal coordinates of the Ath node in the ith degree of freedom at configuration ${}^t\chi$, ${}^i u_A^i$ are the nodal displacements defined in a same manner and N^A is the shape function of the Ath node. The right subrscript A (an uppercase letter) shows the value at node A and follows the summation convention with regard to all nodes connected to an element.

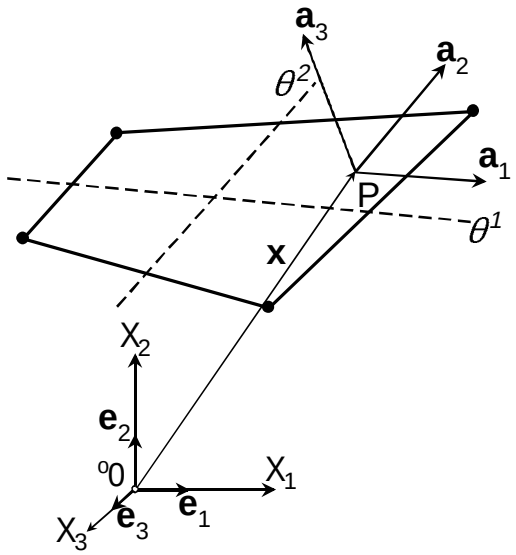

Fig. 19. A typical finite element and the coordinate systems used.

The position vector of any point P on the middle surface can be written with respect to the fixed origin 0 as

$$ {}^t\mathbf{x} = N^A \, {}^t x_A^i \, \mathbf{e}_i \quad , \tag{4.8} $$

where $\mathbf{e}_i$ are the unit base vectors of the fixed rectangular Cartesian coordinates. Differentiating equation (4.8) yields the surface covariant base vector

$$ {}^t\mathbf{a}_\alpha = \frac{\partial \, {}^t\mathbf{x}}{\partial \theta^\alpha} = {}^t a_\alpha^i \, \mathbf{e}_i \quad , \tag{4.9} $$

where

$$ {}^t a_\alpha^i = \frac{\partial N^A}{\partial \theta^\alpha} \, {}^t x_A^i \tag{4.10} $$

yields the Cartesian components of the base vectors. Substituting (4.9) into (3.6) yields the

surface covariant metric tensor for the configuration ${}^t\chi$

$$ {}^t a_{\alpha\beta} = {}^t\mathbf{a}_\alpha \cdot {}^t\mathbf{a}_\beta = \frac{\partial N^A}{\partial \theta^\alpha} \frac{\partial N^B}{\partial \theta^\beta} \; {}^t x_A^{\,i} \; {}^t x_B^{\,i} \; . \tag{4.11} $$

We next introduce finite element matrices to facilitate computer programming. This is done in the same way as Bathe & *et.*. (1975) and Nogushi & Hisada (1995). Interpolations of coordinates, displacement components and components of the base vectors in equations (4.6), (4.7) and (4.10) can be written in a matrix form as components of a global fixed coordinate system

$$ {}^t\mathbf{x} = \boldsymbol{N} \; {}^t\boldsymbol{x} \tag{4.12} $$

$$ \mathbf{u}(\mathbf{x}, t) = \boldsymbol{N} \; \boldsymbol{u} \tag{4.13} $$

$$ {}^t\mathbf{a}_\alpha(\mathbf{x}, t) = \boldsymbol{N}_{,\alpha} \; {}^t\boldsymbol{x} \quad , \tag{4.14} $$

where $\boldsymbol{N}$ is the shape function matrix

$$ \boldsymbol{N} = \left[\begin{array}{ccc|c|ccc|c|ccc} N^1 & 0 & 0 & & N^k & 0 & 0 & & N^N & 0 & 0 \\ 0 & N^1 & 0 & \cdots & 0 & N^k & 0 & \cdots & 0 & N^N & 0 \\ 0 & 0 & N^1 & & 0 & 0 & N^k & & 0 & 0 & N^N \end{array} \right] , \tag{4.15} $$

$\boldsymbol{x}^{\mathrm{T}} = \left\{ x_1^1 \, x_1^2 \, x_1^3 \; \ldots \; x_k^1 \, x_k^2 \, x_k^3 \; \ldots \; x_N^1 \, x_N^2 \, x_N^3 \right\}$ is the column vector containing element nodal coordinates and $\boldsymbol{u}^{\mathrm{T}} = \left\{ u_1^1 \, u_1^2 \, u_1^3 \; \ldots \; u_k^1 \, u_k^2 \, u_k^3 \; \ldots \; u_N^1 \, u_N^2 \, u_N^3 \right\}$ is the column vector containing element nodal displacements referred to the fixed base $\mathbf{e}_i$.

We then construct transformation matrices defining transformations from the displacement vector to the strain in the element. Matrix $\boldsymbol{B}_L$ is the transformation matrix between the nodal displacements $\boldsymbol{u}$ and the column vector of linear strain ${}_t\boldsymbol{\varepsilon}$, i.e.

$$ {}_t\boldsymbol{\varepsilon} = {}^t\boldsymbol{B}_L \; \boldsymbol{u} \; , \tag{4.16} $$

where ${}_t\boldsymbol{\varepsilon}^{\mathrm{T}} = \left\{ {}_t\varepsilon_{11} \;\; {}_t\varepsilon_{22} \;\; 2 \, {}_t\varepsilon_{12} \right\}$ and

$$ {}^{t}\boldsymbol{B}_{L} = \left[\begin{array}{c|c|c} {}^{t}\mathbf{a}_1^{\mathrm{T}} \dfrac{\partial N^1}{\partial \theta^1} & \cdots & {}^{t}\mathbf{a}_1^{\mathrm{T}} \dfrac{\partial N^k}{\partial \theta^1} & \cdots & {}^{t}\mathbf{a}_1^{\mathrm{T}} \dfrac{\partial N^N}{\partial \theta^1} \\ {}^{t}\mathbf{a}_2^{\mathrm{T}} \dfrac{\partial N^1}{\partial \theta^2} & & {}^{t}\mathbf{a}_2^{\mathrm{T}} \dfrac{\partial N^k}{\partial \theta^2} & & {}^{t}\mathbf{a}_2^{\mathrm{T}} \dfrac{\partial N^N}{\partial \theta^2} \\ {}^{t}\mathbf{a}_1^{\mathrm{T}} \dfrac{\partial N^1}{\partial \theta^2} + {}^{t}\mathbf{a}_2^{\mathrm{T}} \dfrac{\partial N^1}{\partial \theta^1} & & {}^{t}\mathbf{a}_1^{\mathrm{T}} \dfrac{\partial N^k}{\partial \theta^2} + {}^{t}\mathbf{a}_2^{\mathrm{T}} \dfrac{\partial N^k}{\partial \theta^1} & & {}^{t}\mathbf{a}_1^{\mathrm{T}} \dfrac{\partial N^N}{\partial \theta^2} + {}^{t}\mathbf{a}_2^{\mathrm{T}} \dfrac{\partial N^N}{\partial \theta^1} \end{array} \right] . \quad (4.17) $$

The nonlinear strain-displacement transformation matrix $\boldsymbol{B}_{NL}$ forms a link between the element's nodal displacements $\boldsymbol{u}$ and the displacement gradients $\boldsymbol{d}$, i.e.

$$ \boldsymbol{d} = \boldsymbol{B}_{NL}\, \boldsymbol{u} \ , \quad (4.18) $$

where $\boldsymbol{d} = \left\{ \dfrac{\partial \mathbf{u}}{\partial \theta^1} \ \dfrac{\partial \mathbf{u}}{\partial \theta^2} \right\}^T$ and

$$ \boldsymbol{B}_{NL} = \left[\begin{array}{ccc|c|ccc|c|ccc} N_{,1}^1 & 0 & 0 & & N_{,1}^k & 0 & 0 & & N_{,1}^N & 0 & 0 \\ 0 & N_{,1}^1 & 0 & & 0 & N_{,1}^k & 0 & & 0 & N_{,1}^N & 0 \\ 0 & 0 & N_{,1}^1 & & 0 & 0 & N_{,1}^k & & 0 & 0 & N_{,1}^N \\ N_{,2}^1 & 0 & 0 & \cdots & N_{,2}^k & 0 & 0 & \cdots & N_{,2}^N & 0 & 0 \\ 0 & N_{,2}^1 & 0 & & 0 & N_{,2}^k & 0 & & 0 & N_{,2}^N & 0 \\ 0 & 0 & N_{,2}^1 & & 0 & 0 & N_{,2}^k & & 0 & 0 & N_{,2}^N \end{array} \right] = \left[\begin{array}{c} \boldsymbol{N}_{,1} \\ \boldsymbol{N}_{,2} \end{array} \right] . \quad (4.19) $$

Moreover, we define the following additional matrices. Material property matrix $\boldsymbol{C}$ is a 3 x 3 matrix

$$ \boldsymbol{C} = \left[\begin{array}{ccc} C^{1111} & C^{1122} & C^{1112} \\ C^{2211} & C^{2222} & C^{2212} \\ C^{1211} & C^{1222} & C^{1212} \end{array} \right] . \quad (4.20) $$

The stress matrix ${}^{t}\boldsymbol{n}$ and the column vector ${}^{t}\hat{\boldsymbol{n}}$ are defined as

$$ {}^{t}\boldsymbol{n} = \begin{bmatrix} {}^{t}n^{11} & {}^{t}n^{12} & 0 & 0 & 0 & 0 \\ {}^{t}n^{21} & {}^{t}n^{22} & 0 & 0 & 0 & 0 \\ 0 & 0 & 0 & 0 & 0 & 0 \\ 0 & 0 & 0 & {}^{t}n^{11} & {}^{t}n^{12} & 0 \\ 0 & 0 & 0 & {}^{t}n^{21} & {}^{t}n^{22} & 0 \\ 0 & 0 & 0 & 0 & 0 & 0 \end{bmatrix} \tag{4.21} $$

and

$$ {}^{t}\hat{\boldsymbol{n}}^{\mathrm{T}} = \left\{ {}^{t}n^{11} \;\; {}^{t}n^{22} \;\; {}^{t}n^{12} \right\}. \tag{4.22} $$

The component matrix of transport velocity $\boldsymbol{v}^{2}$ and the component column vector of transport velocity $\hat{\boldsymbol{v}}^{2}$ are

$$ \boldsymbol{v}^{2} = \begin{bmatrix} v^{1}v^{1} & v^{1}v^{2} & 0 & 0 & 0 & 0 \\ v^{1}v^{2} & v^{2}v^{2} & 0 & 0 & 0 & 0 \\ 0 & 0 & 0 & 0 & 0 & 0 \\ 0 & 0 & 0 & v^{1}v^{1} & v^{1}v^{2} & 0 \\ 0 & 0 & 0 & v^{1}v^{2} & v^{2}v^{2} & 0 \\ 0 & 0 & 0 & 0 & 0 & 0 \end{bmatrix} \tag{4.23} $$

and

$$ \hat{\boldsymbol{v}}^{2^{\mathrm{T}}} = \left\{ v^{1}v^{1} \;\; v^{2}v^{2} \;\; v^{1}v^{2} \right\}. \tag{4.24} $$

The governing finite element equation for a single element can now be derived from (4.5) as

$$ \boldsymbol{M}\,{}^{t+\Delta t}\ddot{\boldsymbol{u}} + \boldsymbol{G}\,{}^{t+\Delta t}\dot{\boldsymbol{u}} + \left[{}^{t}\boldsymbol{K}_{L} + {}^{t}\boldsymbol{K}_{NL} - \boldsymbol{K}_{G} \right] \boldsymbol{u} = {}^{t+\Delta t}\boldsymbol{R} - {}^{t}\boldsymbol{F} + {}^{t}\boldsymbol{F}_{G} \;, \tag{4.25} $$

where $\boldsymbol{M}$ is the consistent mass matrix, $\boldsymbol{G}$ is the skew symmetric gyroscopic inertia matrix and ${}^{t}\boldsymbol{K}_{L}$, ${}^{t}\boldsymbol{K}_{NL}$, $\boldsymbol{K}_{G}$ are the linear, geometric and gyroscopic stiffness matrices, respectively, as given by the equations

$$ \boldsymbol{M} = \int_{{}^{I}A} \boldsymbol{N}^{\mathrm{T}} \, \boldsymbol{N} \;\; {}^{I}\rho \; {}^{I}h \sqrt{{}^{I}a} \; d\theta^{1} \, d\theta^{2} \tag{4.26} $$

and

$$\boldsymbol{K}_G = \int_{{}^I A} \boldsymbol{B}_{NL}^{\mathrm{T}}\, \boldsymbol{v}^2\, \boldsymbol{B}_{NL}\;\; {}^I\rho\; {}^I h\;\; \sqrt{{}^I a}\; d\theta^1 d\theta^2. \tag{4.30}$$

$$\boldsymbol{G} = \int_{{}^I A} v^{\alpha} \left(\boldsymbol{N}^{\mathrm{T}}\, \boldsymbol{N}_{,\alpha} - \boldsymbol{N}_{,\alpha}^{\mathrm{T}}\, \boldsymbol{N} \right) {}^I\rho\; {}^I h \sqrt{{}^I a}\; d\theta^1 d\theta^2 \tag{4.27}$$

$${}^t\boldsymbol{K}_L = \int_{{}^t A} {}^t\boldsymbol{B}_L^{\mathrm{T}}\; {}^t\boldsymbol{C}\; {}^t\boldsymbol{B}_L \sqrt{{}^t a}\; d\theta^1 d\theta^2 \tag{4.28}$$

$${}^t\boldsymbol{K}_{NL} = \int_{{}^t A} \boldsymbol{B}_{NL}^{\mathrm{T}}\; {}^t\boldsymbol{n}\;\; \boldsymbol{B}_{NL} \sqrt{{}^t a}\; d\theta^1 d\theta^2 \tag{4.29}$$

${}^{t+\Delta t}\boldsymbol{R}$, ${}^t\boldsymbol{F}$, ${}^t\boldsymbol{F}_G$ are column vectors of external, internal and gyroscopic forces, of which the first is usually known and latter two are given by

$${}^t\boldsymbol{F} = \int_{{}^t A} {}^t\boldsymbol{B}_L^{\mathrm{T}}\; {}^t\hat{\boldsymbol{n}}\;\; \sqrt{{}^t a}\; d\theta^1 d\theta^2 \tag{4.31}$$

$${}^t\boldsymbol{F}_G = \int_{{}^I A} {}^t\boldsymbol{B}_L^{\mathrm{T}}\; \hat{\boldsymbol{v}}^2\;\; {}^I\rho\; {}^I h \sqrt{{}^I a}\; d\theta^1 d\theta^2. \tag{4.32}$$

Equation (4.25) represents the dynamic equilibrium condition for the discretized structure at time $t+\Delta t$. Since it has unknown quantities with respect to time $t+\Delta t$, it has to be integrated over time, and if we use direct integration methods we can choose from two classes of solution method: explicit methods (Dokanish & Subbaraj 1989) and implicit methods (Subbaraj & Dokanish 1989).

Explicit time integration techniques are methods in which the solution at time $t+\Delta t$ is obtained by considering equilibrium conditions at time t and using difference expressions to approximate the acceleration and velocity vectors in terms of unknown incremental displacement vectors. It should be noted that such integration schemes do not require factorization of a stiffness matrix in the step-by-step solutions and the solution can essentially be carried out at the element level if the mass and damping matrix are diagonal. The computer operations per time step are generally much less laborious for explicit methods than for implicit methods.

The major drawback with explicit methods is their conditional stability, i.e. if the time increment Δt is greater then some critical size Δt_{cr}, any errors, e.g. round off or truncation errors, grow rapidly and eventually lead to meaningless, often unbounded, response calculations. Explicit methods suit particular well for short duration dynamic problems or wave propagation problems in which the frequency content of the response is wide and itself requires a short time step. Good examples are various kinds of crash analysis in which

wave propagation, reflection and diffraction exercise an important influence.

In implicit time integration techniques the solution at time $t+\Delta t$ requires consideration of the equilibrium condition at time $t+\Delta t$, and therefore the determination of displacement at $t+\Delta t$ involves factorization of the structural stiffness matrix at every time step. Although implicit methods require much more computing for each time step, by choosing an unconditionally stable scheme we can use much larger time steps than with explicit schemes. Only requirement for a time step is that it should be small enough for the response in all modes which significantly contribute to ensuring that the total structural response is calculated accurately. In nonlinear analysis it is usually necessary to perform additional equilibrium iterations in order for the displacements and stresses to satisfy fully the nonlinear conditions of the problem.

Implicit schemes clearly suit the problem considered in this work better than do explicit ones. Since our aim is to determine a frequency response with time integration, we try to achieve a steady state by allowing the transient effect to be damped. The analysis is long and the frequency content of the response is close to the desired natural frequency. Moreover, whereas in explicit schemes any errors admitted in the incremental solution can grow in a path-dependent manner at any subsequent time, the equilibrium iterations in implicit schemes prevent any accumulation of errors (Koivurova 1993).

We will use a Newmark implicit method to integrate the equation (4.25). The following finite difference expansions are employed:

$$\begin{aligned} {}^{t+\Delta t}\boldsymbol{u} &= {}^{t}\boldsymbol{u} + {}^{t}\dot{\boldsymbol{u}}\,\Delta t + \left[\left(\frac{1}{2}-\alpha\right){}^{t}\ddot{\boldsymbol{u}} + \alpha\,{}^{t+\Delta t}\ddot{\boldsymbol{u}}\right](\Delta t)^2 \\ {}^{t+\Delta t}\dot{\boldsymbol{u}} &= {}^{t}\dot{\boldsymbol{u}} + \left[(1-\delta){}^{t}\ddot{\boldsymbol{u}} + \delta\,{}^{t+\Delta t}\ddot{\boldsymbol{u}}\right]\Delta t \quad , \end{aligned} \tag{4.33}$$

where α and δ are integration parameters selected to obtain the best stability and accuracy characteristics in the integration scheme. The parameters in following analyses are chosen to be $\delta = 0.5(1+2\gamma)$ and $\alpha = 0.25(1+\gamma^2)$, where γ is termed the amplitude decay factor.

Solving equation (4.33)[1] for ${}^{t+\Delta t}\ddot{\boldsymbol{u}}$ in terms of ${}^{t+\Delta t}\boldsymbol{u}$ and then substituting ${}^{t+\Delta t}\ddot{\boldsymbol{u}}$ into (4.33)[2], we obtain equations for ${}^{t+\Delta t}\ddot{\boldsymbol{u}}$ and ${}^{t+\Delta t}\dot{\boldsymbol{u}}$, each in terms of the unknown displacement increment $\boldsymbol{u}$ only. These two relations for ${}^{t+\Delta t}\dot{\boldsymbol{u}}$ and ${}^{t+\Delta t}\ddot{\boldsymbol{u}}$ are substituted in equation (4.25), yielding

$$\begin{aligned} \left[\frac{1}{(\alpha\Delta t)^2}\boldsymbol{M} + \frac{\delta}{\alpha\Delta t}\boldsymbol{G} + {}^{t}\boldsymbol{K}\right]\boldsymbol{u} &= {}^{t+\Delta t}\boldsymbol{R} + \boldsymbol{M}\left[\frac{1}{\alpha\Delta t}{}^{t}\dot{\boldsymbol{u}} + \left(\frac{1}{2\alpha}-1\right){}^{t}\ddot{\boldsymbol{u}}\right] + \\ &\quad + \boldsymbol{G}\left[\left(\frac{\delta}{\alpha}-1\right){}^{t}\dot{\boldsymbol{u}} + \frac{\Delta t}{2}\left(\frac{\delta}{\alpha}-2\right){}^{t}\ddot{\boldsymbol{u}}\right] - {}^{t}\boldsymbol{F} + {}^{t}\boldsymbol{F}_{\boldsymbol{G}} \quad , \end{aligned} \tag{4.34}$$

which can be solved for the incremental displacement $\boldsymbol{u}$. As we are considering nonlinear analysis, equilibrium iteration is performed in each time step. The Newton-Raphson iteration schema will be used, which yields following equations

$$\boldsymbol{M}\,{}^{t+\Delta t}\ddot{\boldsymbol{u}}^{(k)} + \boldsymbol{G}\,{}^{t+\Delta t}\dot{\boldsymbol{u}}^{(k)} + {}^{t+\Delta t}\boldsymbol{K}^{(k)}\boldsymbol{u}^{(k)} = {}^{t+\Delta t}\boldsymbol{R} - {}^{t+\Delta t}\boldsymbol{F}^{(k-1)} + {}^{t+\Delta t}\boldsymbol{F}_{\boldsymbol{G}}{}^{(k-1)} \quad , \tag{4.35}$$

where the right superscript k denotes the iteration number. The iteration continues until the appropriate termination criteria are met.

4.2. Fluid-structure interaction

The pressure-based formulation for fluid domain in a fluid-structure interaction analysis expresses the unknown acoustic pressure within a three-dimensional element in terms of the pressure values at the nodes, as follows:

$$p(\theta^1,\theta^2,\theta^3,t) = N^A(\theta^1,\theta^2,\theta^3)\ P_A(t)\ , \tag{4.36}$$

where N^A are a set of linear shape functions and P_A are nodal pressures. Substituting the pressure expression into the acoustic wave equation (2.19) and applying Galerkin's weight residual, the finite element procedure leads to the following matrix equation for the fluid mesh (Woyak 1992):

$$\boldsymbol{M}_f\ \ddot{\boldsymbol{P}} + \boldsymbol{C}_f\ \dot{\boldsymbol{P}} + \boldsymbol{K}_f\ \boldsymbol{P} = \boldsymbol{F}_f\ , \tag{4.37}$$

where $\boldsymbol{M}_f$ = the fluid equivalent "mass" matrix
$\boldsymbol{C}_f$ = the fluid equivalent "damping" matrix
$\boldsymbol{K}_f$ = the fluid equivalent "stiffness" matrix
$\boldsymbol{F}_f$ = the "fluid load" vector applied.

The coupling of fluid-structure interaction at the interface will be achieved with the approximation of equation (2.20). Because of interaction at the interface boundary, an acoustic pressure $\boldsymbol{R}\ \boldsymbol{P}$ is exerted on to the membrane and the motions of the membrane produce an effective fluid load $\rho_o\ \boldsymbol{R}\ \ddot{\boldsymbol{u}}$. The matrix $\boldsymbol{R}$ is a coupling matrix that represents the effective surface area associated with each node on the fluid-structure interface. These unknown interface "load" quantities are added to the finite element equation for the membrane (4.25) and the fluid domain (4.37). These two equations can be combined into a single equation to produce the following form (Woyjak 1992):

$$\begin{bmatrix} \boldsymbol{M} & 0 \\ \rho_o \boldsymbol{R}^T & \boldsymbol{M}_f \end{bmatrix} \begin{Bmatrix} \ddot{\boldsymbol{u}} \\ \ddot{\boldsymbol{P}} \end{Bmatrix} + \begin{bmatrix} \boldsymbol{G} & 0 \\ 0 & \boldsymbol{C}_f \end{bmatrix} \begin{Bmatrix} \dot{\boldsymbol{u}} \\ \dot{\boldsymbol{P}} \end{Bmatrix} + \begin{bmatrix} \boldsymbol{K} & -\boldsymbol{R} \\ 0 & \boldsymbol{K}_f \end{bmatrix} \begin{Bmatrix} \boldsymbol{u} \\ \boldsymbol{P} \end{Bmatrix} = \begin{Bmatrix} \boldsymbol{F} \\ \boldsymbol{F}_f \end{Bmatrix}. \tag{4.38}$$

4.3. Implementation in a FEM program

The model of an axially moving membrane was implemented to a general FEM program, ANSYS (ANSYS 5.2 1994) as a programmable user element (Koivurova 1996). As the ANSYS program has a membrane element SHELL 41 which includes geometrically nonlinear effects, the influences of the deformations developing after the initial state are calculated with this. The user element GYRO100 is used to considering the gyroscopic effects and the geometrical stiffness arising from the initial tension. The equation of motion (4.25) is divided into two parts, an initial, gyroscopic part, which includes the effects of initial tension and axial motion,

$$\boldsymbol{G}^{t+\Delta t}\ddot{\boldsymbol{u}}_n + \left[{}^{I}\boldsymbol{K}_{NL} - \boldsymbol{K}_G\right]\boldsymbol{u}_n = -{}^{I}\boldsymbol{F} + {}^{t}\boldsymbol{F}_G \ , \tag{4.39}$$

and a membrane configuration part,

$$\boldsymbol{M}^{t+\Delta t}\ddot{\boldsymbol{u}}_n + \left[{}^{t}\boldsymbol{K}_L + {}^{I\to t}\boldsymbol{K}_{NL}\right]\boldsymbol{u}_n = {}^{t+\Delta t}\boldsymbol{R} - {}^{I\to t}\boldsymbol{F}. \tag{4.40}$$

Here the geometrical stiffness matrix and the internal force vector are separated by splitting the tension into two parts:

$${}^{t}\boldsymbol{n} = {}^{I}_{t}\tilde{\boldsymbol{n}} + {}^{I\to t}_{t}\tilde{\boldsymbol{n}} \ , \tag{4.41}$$

the initial tension ${}^{I}_{t}\tilde{\boldsymbol{n}}$ and the tension ${}^{I\to t}_{t}\tilde{\boldsymbol{n}}$ (= ${}^{I\to t}\boldsymbol{n}$) developing during deformation after the initial state. This leads, through the transformation (3.3) to the following geometric stiffness matrices:

$$\begin{aligned} {}^{t}\boldsymbol{K}_{NL} &= \int_{{}^{I}A} \boldsymbol{B}_{NL}^{\mathrm{T}}\ {}^{I}\boldsymbol{n}\ \boldsymbol{B}_{NL}\ d\,{}^{I}A + \int_{{}^{t}A} \boldsymbol{B}_{NL}^{\mathrm{T}}\ {}^{I\to t}\boldsymbol{n}\ \boldsymbol{B}_{NL}\ d\,{}^{t}A \\ &= {}^{I}\boldsymbol{K}_{NL} + {}^{I\to t}\boldsymbol{K}_{NL} \end{aligned} \tag{4.42}$$

and the following internal force vectors:

$$\begin{aligned} {}^{t}\boldsymbol{F} &= \int_{{}^{I}A} \boldsymbol{B}_{NL}^{\mathrm{T}}\ {}^{I}\hat{\boldsymbol{n}}\ d\,{}^{I}A + \int_{{}^{t}A} \boldsymbol{B}_{NL}^{\mathrm{T}}\ {}^{I\to t}\hat{\boldsymbol{n}}\ d\,{}^{t}A \\ &= {}^{I}\boldsymbol{F} + {}^{I\to t}\boldsymbol{F}. \end{aligned} \tag{4.43}$$

The element model should generate these two types of element one on the other at the same degrees of freedom.

The use of convected coordinates entails us several advantages in the implementation. If we specify our convected coordinates θ^1, θ^2 to be nondimensional isoparametric natural coordinates of a membrane element, the element equations are simplified, as there is no need to perform any coordinate transformations. Moreover, although gyroscopic matrices are nonlinear, they can be written as constant matrices because of the conservation of mass and the fact that the convective components of transport velocity are constants. Therefore there is no need to update the gyroscopic inertia and gyroscopic stiffness matrix during an

analysis.

5. Results

5.1. Linear eigenvalue analysis of an axially moving simply supported membrane in surrounding air

Verification of the overall accuracy of the model is quite difficult, because there are only a few experimental results, which consider an axially moving membrane and these are limited to the linear range. Pramila (1986) measured fundamental frequencies for a narrow paper web with a length of L = 2.4 m, a width of b = 0.47 m and a mass per unit area of m = 35 g/m^2. These values are used in the finite element model of the present eigenvalue analysis shown in Fig. 20. The surrounding air is modelled here with acoustic fluid elements, and the density of air is taken to be 1.3 kg/m^3. The dimensions and boundary conditions of the air domain are those given in Niemi & Pramila (1987) and the parameters used are listed in Table 1.

Table 1. Calculation parameters.

length	L	=	2.4	m
width	b	=	47	cm
thickness	h	=	0.49	mm
mass per unit area	m	=	35	g/m^2
initial tension	${}^{I}n_{11}$	=	362	N/m
elastic modulus	E	=	1*10^9	N/m^2

The results of the eigenvalue analysis and the experiments performed by Pramila (1986) are shown in Fig. 21. The two dashed lines represent the analytical results of Pramila (1987) in which the surrounding air is described by means of two added mass models. For the sake of clarity, the results are shown nondimensionally in the form of frequency and transport velocity. They are defined as follows:

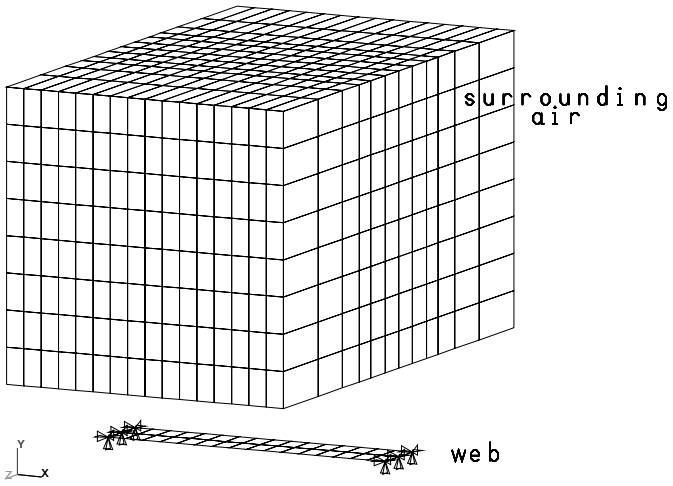

Fig. 20. FE-model of fluid domain and web.

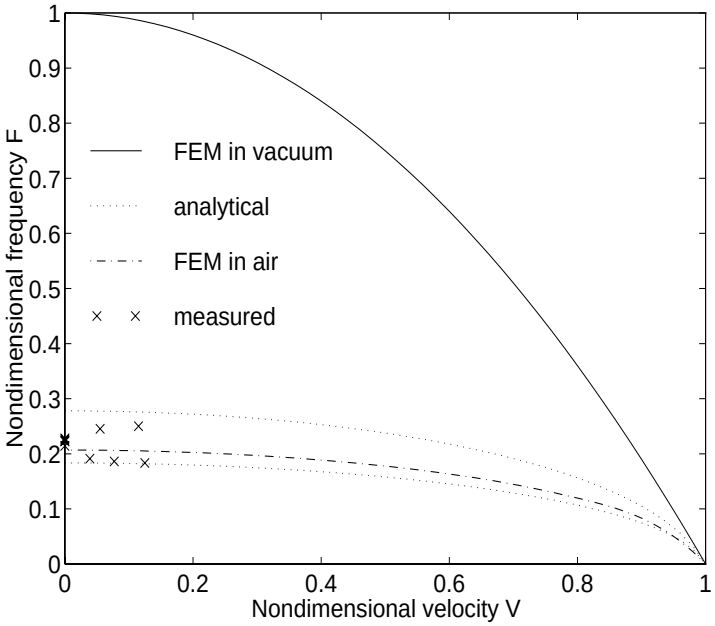

Fig. 21. Nondimensional fundamental frequency as a function of velocity, mass per unit area = 35 g/m^2.

$$F = f\,2L\sqrt{\frac{m}{{}^{I}n_{11}}} \tag{5.1}$$

$$V = v\sqrt{\frac{m}{{}^{I}n_{11}}} \tag{5.2}$$

The same nondimensional presentation is used for all the following analyses. The results shown in Fig. 21 are in good agreement when the interaction with air is taken into account. Experimental verification in the nonlinear range is not possible, because the pilot paper mill used by Pramila (1986) limited its experiments to the linear range.

5.2. Nonlinear analysis of an axially moving membrane in comparison with an axially moving string

Although it is not possible to make comparisons with any experimental results in the nonlinear range, it is quite interesting to compare results calculated here with analytical and numerical analyses performed for an axially moving nonlinear string by Wickert (1992), who studied a travelling beam and string with a second-order perturbation solution by the asymptotic method of Krylov, Bogoliubov and Mitropolsky and made comparisons with the results of numerical integration and some other studies.

Table 2. Calculation parameters.

length	L	=	1.0	m
width	b	=	40	mm
thickness	h	=	1.0	mm
mass per unit area	m	=	250	g/m^2
initial tension	${}^{I}n_{11}$	=	2500	N/m
elastic modulus	E	=	1*10^9	N/m^2

The fundamental frequency of an axially moving nonlinear membrane is calculated by transient time integration from dynamic response history by taking the initial conditions for a nonlinear resonance vibration study. The initial displacement and velocity vectors are proportional to the normalized nonlinear response of the asymptotic solution calculated by Wickert (1992). The parameters for the analysis are chosen so the that multiplier $\varepsilon a_0 v_l = 0.25$, where ε is a perturbation coefficient (= 0.7), a_0 is a nondimensional amplitude

of vibration (= A/L = 0.018) and v_l is a longitudinal stiffness parameter (= $\sqrt{E\,h/n_{11}}$ = 20). The other calculation parameters are set out in Table 2.

The FEM results for fundamental frequency are compared with the results obtained from Wickert (1992) in Table 3 and Fig. 22. The present solutions agree to within 3 % with both the asymptotic and numerical integration solutions for V $\leq$ 0.8 (Wickert 1992) and for V $\leq$ 0.6 (Thurman and Mote 1969). At higher speeds the difference relative to the results of Wickert increases rapidly. An explanation for the difference could be sought from two sources. Wickert (1992) used a stretching approximation for the longitudinal direction in which he proposes that the longitudinal displacement field

$$u_x(x,t) = \frac{x}{2}\int_0^1 \frac{\partial u_y^2}{\partial x}\,dx - \frac{1}{2}\int_0^x \frac{\partial u_y^2}{\partial x}\,dx \tag{5.3}$$

arises entirely from finite transverse vibration. It was not possible to validate this approximation with the non-approximated results of Thurman and Mote (1969) for the region 0.6 < V $\leq$ 1. Moreover, as Wickert (1992) concludes, the inclusion of nonlinearity in vibration studies is most important at a near-critical speed $v_{cr} = \sqrt{n_{11}/m}$, where modal stiffness is small and is dominated by nonlinear extensional stiffness. Another explanation for the difference in the results at a near-critical speed could be the fact that Wickert (1992) does not take into account the change in transport velocity due to the deformation.

Table 3. Comparison of linear and nonlinear fundamental frequency calculations for an axially moving membrane and string with $\varepsilon a_0 v_l = 0.25$.

Nondimensional speed V	0	0.2	0.4	0.6	0.8	1
Linear	1	0.96	0.84	0.64	0.36	0
FEM solution for membrane	1.11	1.07	0.96	0.78	0.55	0.25
Integration (Wickert 1992)	1.109	1.069	0.955	0.78	0.558	0.308
Asymptotic (Wickert 1992)	1.112	1.077	0.966	0.792	0.569	0.308
Thurman and Mote (1969)	1.103	1.067	0.955	0.77	-	-

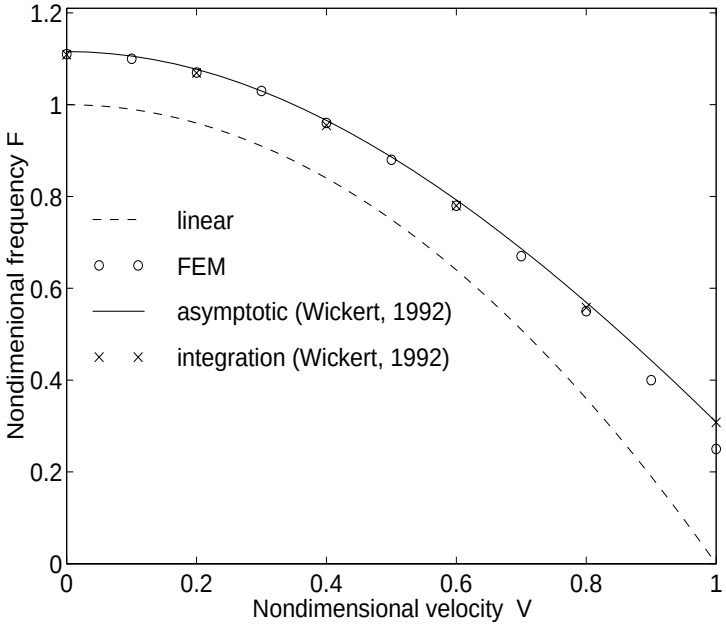

Fig. 22. Comparison of linear and nonlinear fundamental frequency calculations for an axially moving membrane and string with $\varepsilon a_0 v_l$ = 0.25.

5.3. Nonlinear vibration of a simply supported axially moving band without the surrounding air

The nonlinear dynamic behaviour of an axially moving membrane is examined through the response resulting from harmonic boundary excitation. The response is calculated by direct time integration of equations of motion for each frequency until the steady state is obtained. The method requires a lot of computer time, but because we wanted to include the contact between the membrane and the rolls, it was very probably impossible to use other methods such as the harmonic balance and perturbation.

We consider first a narrow band with fixed simple supports but no supporting rolls. A typical harmonic response curve for the present nonlinear system at an transport velocity of 50% of the critical value $v_{cr} = \sqrt{n_{11}/m}$ is shown in Fig. 23. The amplitude of the harmonic boundary motion is 2.4 mm and the other calculation parameters used for the geometry and the material are as in Table 4. The element model is the web part shown in Fig. 20.

A typical response curve for harmonic excitation of a nonlinear system will look like that shown in Fig. 23, determined by observing the amplitude of the steady state vibration of a

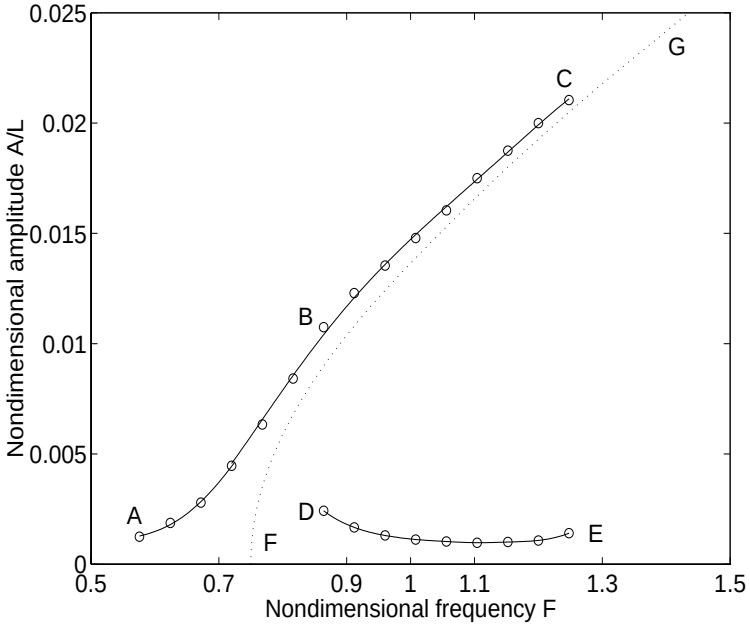

Fig. 23. Nondimensional mid-span response amplitude for a membrane exited near to its fundamental frequency. Transport velocity is 50% of the critical value.

midpoint *A* at different excitation frequencies *f* (Fig. 24). As can be seen in Fig. 23, the harmonic response of a nonlinear system is a frequency range in which two possible steady state solutions exist. Which one is actually achieved will depend on the initial state. These analyses employed two sets of initial conditions:

(I) a straight configuration and zero initial velocity in a low frequency range from A to B and a higher range from D to E, and

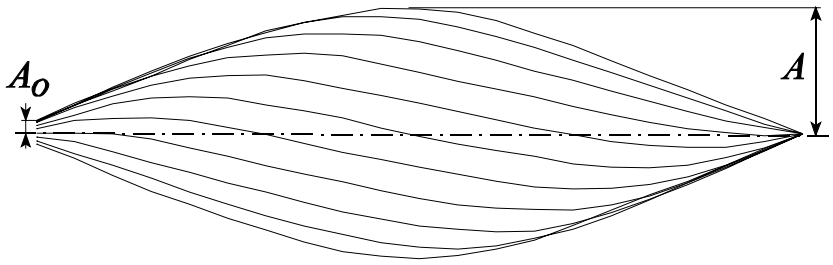

Fig. 24. Half-period of steady state vibration (F=0.816, A_o/L = 0.001, V=0.5).

(II) an extreme position of linear eigenvibration in the range between B and C

The curve FG in Fig. 23 is a backbone curve calculated in a same way as the frequency - transport velocity relationship in Fig. 22.

Table 4. Calculation parameters.

length	L	=	2.4	m
width	b	=	47	cm
thickness	h	=	0.49	mm
mass per unit area	m	=	35	g/m^2
initial tension	${}^{I}n_{11}$	=	362	N/m
elastic modulus	E	=	1*10^9	N/m^2
amplitude of boundary motion	A_o	=	2.4	mm

In this kind of analysis, if there is no internal damping present, it is impossible to reach the steady state and damp the transient effect out (Kanarachos & Spentzas 1988). Thus artificial damping is used to shorten the analysis. The damping used varies with time as shown in Fig 25 and is proportional to the linear stiffness matrix of the membrane with parameter D. The value of the damping coefficient was determined so that the steady state would be achieved after 50 - 70 vibration periods (see Fig. 26). The maximum value D varies in the range 0 - 0.009 depending on the vibration amplitude and other parameters.

The response curves were calculated for four axial velocities, 0%, 50%, 70% and 90% of the critical velocity $v_{cr} = \sqrt{n_{11}/m}$. The response-frequency curves of Fig. 27 show that the system behaves like a nonlinear hard spring. The nonlinearity clearly stiffens the system as the amplitude increases and this effect seems to be accentuated slightly with the increase in transport velocity. According to Wickert (1992) in his analysis of a nonlinear string and beam, the same phenomenon could be caused by a decrease in modal stiffness. If we compare these nonlinear responses with the linear ones in Fig. 28, where the dash-dot lines are the results of linear analysis, we see behaviour typical of nonlinear systems, a jump to the next mode. For an axially moving membrane this can take place to the next mode but one, the next but two etc. when the transport velocity is high enough.

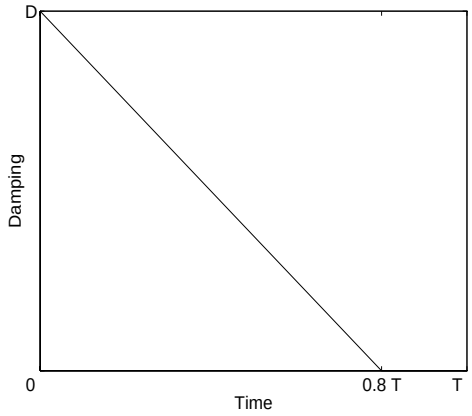

Fig. 25. Artifical damping as a function of time.

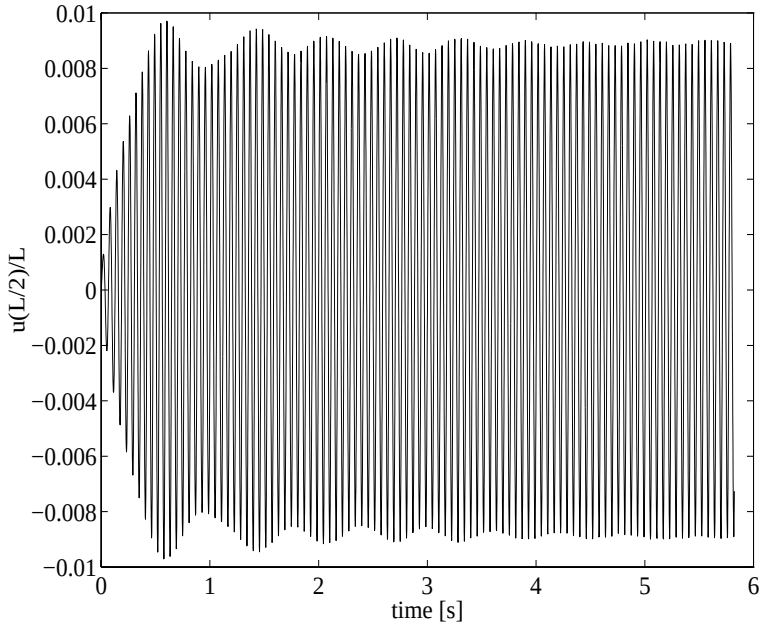

Fig. 26. Transverse motion of the midpoint (F=0.816, A_o/L = 0.001, V=0.5).

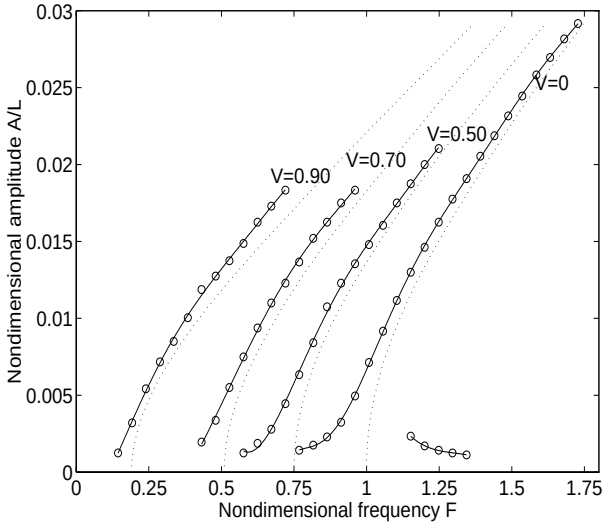

Fig. 27. Nondimensional mid-span response amplitude for an axially moving membrane travelling at velocities of 0%, 50%, 70% and 90% of the critical value.

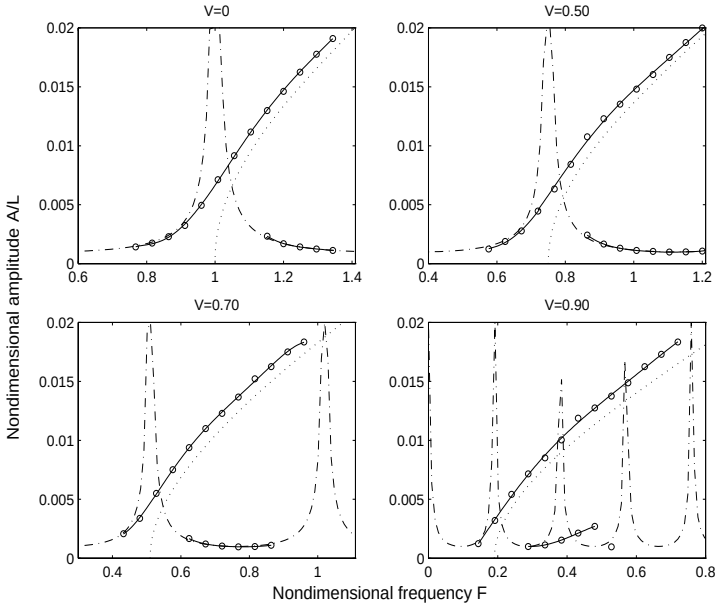

Fig. 28. Comparison of linear (-··-) and nonlinear (—) mid-span response amplitudes for an axially moving membrane travelling at velocities of 0%, 50%, 70% and 90% of the critical value.

5.4. Nonlinear vibration of a band travelling between two cylinders without the surrounding air

In order to obtain an insight into the influence of supporting rolls, we developed a model of a narrow web moving over the open draw of two finite cylinders, as shown in Fig. 29. The dynamic behaviour of the system was analyzed in the same way as in the previous example. Harmonic boundary excitation was applied to one cylinder and the variations in response are observed at different excitation frequencies. The support cylinders are modelled as rigid ones and their radii are chosen to be a half and a quarter of the length of the free span. The contact between the cylinders and the paper web is assumed to be frictional, with a friction coefficient = 0.4. If we look at the frequency response curves in Fig. 30 and compare the results with those for the system with a support cylinder and that with simple boundaries, we see a clear difference. The frequency response curves in Fig. 30 and 31 show that the support cylinders reduce the effect of the nonlinearity. Using the radius of the cylinder as a parameter, we see that as the radius grows the effect of the cylinder increases. The same happens with the decrease in the coefficient of friction in Fig. 31. The reason for this behaviour seems to be movement of the boundary point and sliding of the membrane on the cylinders. It can be concluded that the importance of the effects of supporting rolls on the system depends on the geometry (radius of the cylinders) and the roughness of the contact surfaces (friction coefficient).

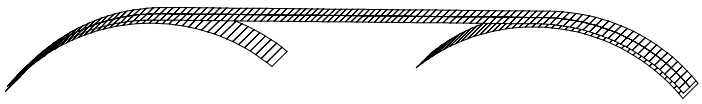

Fig. 29. FE model of a web and contacting cylinders.

5.5. Nonlinear vibration of an axially moving simple supported membrane in surrounding air

The effect of the surrounding air on a nonlinear model was considered using the same element model as in the above eigenvalue analysis (see Fig. 20). The parameters are otherwise the same as in the previous example, only the mass per unit area has been altered to 53 g/m^{2}.

The frequency - transport velocity relationships are estimated from the dynamic response history by taking the initial conditions for the nonlinear resonance vibration study.

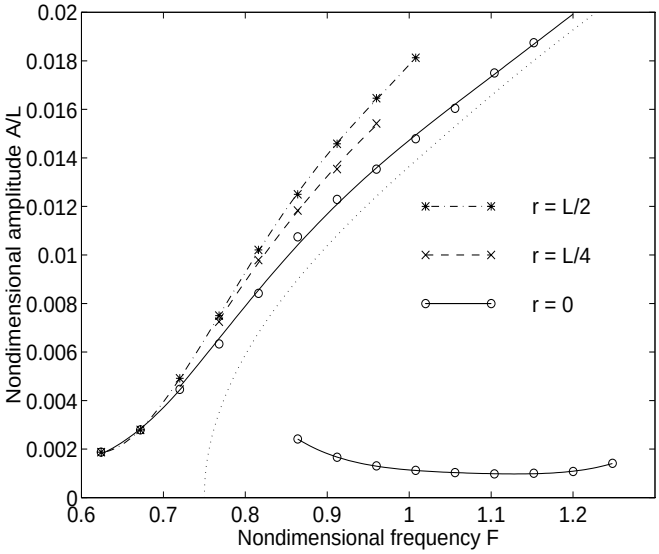

Fig. 30. Comparison of mid-span frequency responses for a membrane with supporting rolls of radius *L*/2, *L*/4 and 0 (fixed ends). (*V* = 0.5 and μ = 0.4).

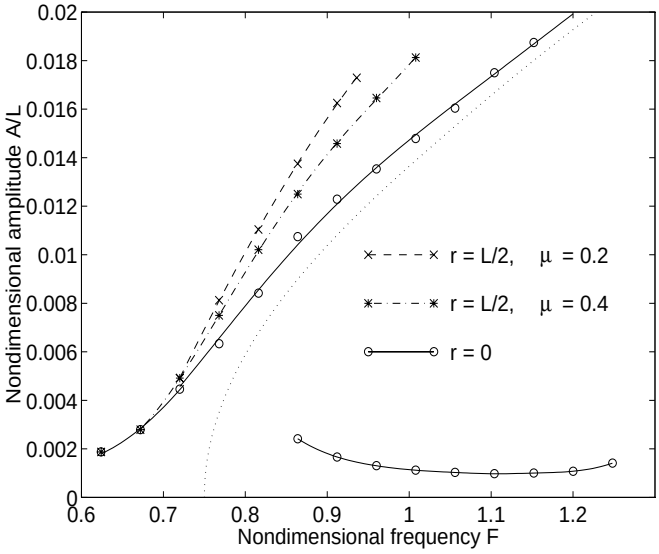

Fig. 31. Comparison of mid-span frequency responses for a membrane when the friction coefficient varies from 0.2 to 0.4. (*V* = 0.5 and *r* = L/2).

The initial displacement and velocity vectors are proportional to the normalized linear eigenmode vectors. The backbone curves in Fig. 23, 27, 28, 30 and 31 above were determined in the same way.

The results in Fig. 32 show the same behaviour as mentioned by Wickert (1992) for axially moving strings and beams. The influence of the nonlinearity is most significant near the critical velocity, where the modal stiffness is small. We can also see that the surrounding air is as important in nonlinear analysis as it is in eigenvalue analysis.

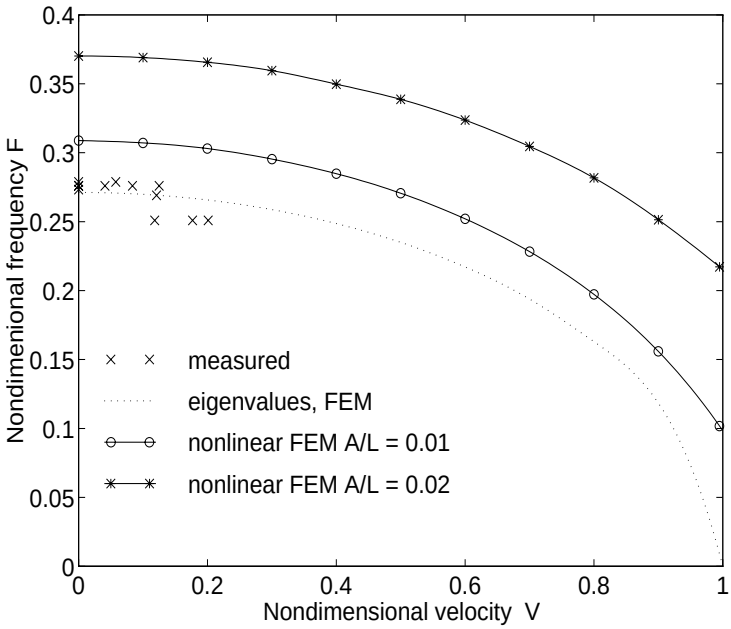

Fig. 32. Fundamental frequency as a function of velocity obtained by linear and nonlinear analysis, mass per unit area = 53 g/m^2.

6. Conclusions

A geometrically nonlinear theory for behaviour of an axially moving membrane has been presented here. The model is based on convected coordinate formulation, mixed description of the initially stressed continuum and Hamilton's principle. The formulation includes geometrical nonlinearities, i.e. large displacement, variation in tension along the membrane, variation in transport velocity due to deformation and contact with a supporting structure. By making additional adequate assumptions regarding the initial state and the size of the displacements, this formulation leads to the linear equation of motion derived by Niemi & Pramila (1987) as a special case.

For applications of the theoretical model a novel numerical formulation for an axially moving membrane is introduced. The special choice of a convected coordinate system in the reference configuration leads to a formulation which significantly simplifies the equations in both the theoretical and the numerical formulation:

(I) Incremental displacement and the convected base in the initial state appear in vector form.
(II) The change in transport velocity can be taken into account by the constant components of the convected base.
(III) Numerical implementation is simple and leads to element equations with a few arithmetic operations. The gyroscopic inertia and stiffness matrix do not need updating as they would if Cartesian coordinates were used. Also, there are fewer transformations between coordinate systems than in a standard formulation.

Verification of the model against experimental results was possible in the linear range. The nonlinear dynamic behaviour of the membrane was examined and the influence of contact between it and supporting cylinders and interaction between it and the surrounding air were studied by determining the responses resulting from harmonic boundary excitation. The harmonic response was determined by time integration of equations in the motion of finite element model, as other methods would have been very difficult or impossible. Time integration was time-consuming, because it required 50 - 70 vibration periods to achieve a steady state even if artificial damping was used. Also, the contact algorithm needs very short time steps and several equilibrium iterations. Maximum cpu time for a SGI Power Onyx R8000 machine was about 120 000 seconds for one point in a harmonic response

curve. The analysis was also demanding in other respect because the convergence of the solution was weak and sensitive for selection of initial values and the coefficient of artificial damping.

The results achieved show clearly that nonlinearities cause a considerable stiffening of the membrane and the fundamental frequency increases as the amplitude grows.
The effects are accentuated slightly as the transport velocity increases. According to Wickert (1992), reason for this is a decrease in modal stiffness as the velocity increases, while the influence of the nonlinearity is growing at the same time.

The results also show that the cylindrical supports have considerable influence on the behaviour of an axially moving membrane. The boundary of the contact region clearly moves and the membrane slides on the cylinders. This weakens the nonlinear hardening phenomena and lowers the fundamental frequency. This influence gains in strength as the radius of the cylinder increases, or if the friction coefficient decreases. The surrounding air has the same kind of effect on the dynamic behaviour in nonlinear analysis as is observed in eigenvalue analysis.

References

Ames W F, Lee S Y & Zaiser J N (1968) Nonlinear vibration of a travelling threadline. International Journal of Nonlinear Mechanics 3: 449-469.

ANSYS 5.2 (1994) User manual volume IV, theory. Swanson Analysis Systems Inc.

Arbate S (1992) Vibrations of belts and belt drives. Mechanisms and Machines Theory 27: 645–659.

Bathe K J (1982) Finite Element Procedures in Engineering Analysis. Presentice Hall, Englewood Cliffs, New Jersey.

Bathe K J, Ramm E & Wilson E L (1975) Finite element formulations for large deformation dynamic analysis. International Journal for Numerical Methods in Engineering 9: 353-386.

Benjamin T B (1961) Dynamics of a system of articulated pipes conveying fluid - part I theory, and part II experiments. Proceedings of Royal Society 261: 457-499.

Chang Y B (1990) An experimental and analytical study of web flutter. Ph.D. Dissertation Oklahoma State University.

Dokainish M A & Subbaraj K A (1989) Survey of direct time-integration methods in computational structural dynamics-I. Explicit methods. Computers & Structures 32: 1371-1386.

Green A E & Zerna W (1968) Theoretical Elasticity. Clarendon Press, Oxford.

Hwang S J & Perkins N C (1992a) Supercritical stability of an axially moving beam part I: model and equilibrium analysis. Journal of Sound and Vibration 154: 381-396.

Hwang S J & Perkins N C (1992b) Supercritical stability of an axially moving beam part II: vibration and stability analysis. Journal of Sound and Vibration 154: 397-409.

Kanarachos A E & Spentzas C N (1988) An artificial damping method for the determination of te steady state of harmonically excited nonlinear systems. Journal of Sound and Vibration 120: 597-608.

Kim Y & Tabarrok B (1972) On the nonlinear vibration of travelling string. Journal of The Franklin Institute 293: 381-399.

Kleiber M (1989) Incremental Finite Element Modelling in Nonlinear Solid Mechanics. Ellis Horwood, Chichester.

Koivurova H (1996) Vibration of axially moving membrane by ANSYS. In: Ashraf A. (ed.): The Future Simulation Tools: Computer Aided Engineering in the 21st Century. Ansys, Pittsburgh, p 3.109-3.116.

Koivurova H (1995) Dynamic contact analysis of axially moving membrane and guiding structure with element method. Unpublished licentiate thesis, University of Oulu.

Koivurova H (1993) Vibration of axially moving narrow membrane travelling between two roll-supports having finite radius. In: Aliabadi, M. H. & Brebbia, C. A. (ed.) Contact Mechanics-Computational Techniques. Computational Mechanics Publications Inc. Southampton, p 11-18.

Koivurova H & Pramila A (1997) Nonlinear vibration of axially moving membrane by finite element method. Computational Mechanics 20: 573 - 581.

Laukkanen J (1995) Numerical analysis of vibration of an axially moving membrane and surrounding air. Unpublished licentiate thesis, University of Oulu.

Laukkanen J & Pramila A. (1997) FEM analysis of a travelling paper web and surrounding air. In: Godoy L A, Rysz M & Suarrez L E (ed) Applied Mechanics in the Americas, vol 4: Mechanics and Dynamics of Solids. The University of Iowa, Iowa City, p 505-508.

Lee S (1966) Wave propagation and vibration of a string undergoing axial motion. Ph.D. Dissertion, University of Delaware.

Luongo A, Rega G & Vestroni F (1984) Planar nonlinear free vibrations of an elastic cable. International Journal of NonLinear Mechanics 19: 39-52.

Malvern L E (1969) Introduction to the Mechanics of a Continuous Medium. Prentice-Hall, New Jersey.

McIver D B (1973) Hamilton's principle for systems of changing mass. Journal of Engineering Mathematics 7: 249-261.

Mote C D Jr (1966) On the nonlinear oscillation of an axially moving string. Journal of Applied Mechanics 33: 463-464.

Mujandar A S & Douglas W J M (1976) Analytical modelling of sheet Flutter. Svenska Pappertidning 79: 187-192.

Nayfeh A H & Mook D T (1979) Nonlinear Oscillations. John Wiley, New York.

Niemi J & Pramila A (1987) FEM-analysis of transverse vibration of an axially moving membrane immersed in ideal fluid. International Journal for Numerical Methods in Engineering 24: 2301-2313.

Niordson F I (1985) Shell Theory. North-Holland, Amsterdam.

Noguchi H & Hisada T (1995) Integrated FEM formulation for Total/Updated-Lagrangian method in geometrically nonlinear problems. International Journal JSME Series A 38: 23-29.

Païdoussis M P & Li G X (1993) Pipes conveying fluid: a model dynamical problems. Journal of Fluid and Structures 7: 137-204.

Perkins N C (1989) Asymptotic analysis of a translating cable arch. Journal of Sound and Vibration 135: 375-383.

Perkins N C & Mote C D Jr (1989a) Theoretical and experimental stability of two translating cable equilibria. Journal of Sound and Vibration 128: 397-410.

Perkins N C & Mote C D Jr (1987) Three-dimensional vibration of travelling elastic cables. Journal of Sound Vibration 114: 325-340.

Popov V V (1986) Vibrations of a segment of a variable-length longitudinally-moving string. Prikl. Matem. Mekhan. 50: 161-164.

Pramila A (1987) Natural frequencies of a submerged axially moving band. Journal of Sound Vibration 113: 198-203.

Pramila A (1986) Sheet flutter and the interaction between sheet and air. TAPPI- Journal 69: 70-74.

Rajakumar C & Ali A (1993) Acoustic boundary element eigenproblem with sound absorption and its solution using Lanczos algorithm. International Journal for Numerical Methods in Engineering 36: 3957-3972.

Reismann H & Pawlik P (1977) Dynamics of initially stressed hyperelastic solids. SM Archives 2: 129-185.

Salonen E M (1998) Comments on paper: Perkins & Mote (1987). Private communication.

Subbaraj K & Dokainish M A (1989) A survey of direct time-integration methods in computational structural dynamics-II. Implicit methods. Computers & Structures 32: 1387-1401.

Tagata G (1983) A parametrically driven harmonic analysis of a nonlinear stretched string with time-varying length. Journal of Sound and Vibration 87: 493-511.

Thompson J M & Stewart H B (1986) Nonlinear Dynamics and Chaos. John Wiley, New York.

Thurman A L & Mote C D Jr (1969) Free, periodic, nonlinear oscillation of an axially moving strip. Journal of Applied Mechanics 36: 83-91.

Ulsoy A G & Mote C D Jr (1982): Vibration of wide band saw blades. Journal of Engineering Industry 104: 71-78.

Wickert J A (1992) Nonlinear vibration of a travelling tensioned beam. International Journal of Nonlinear Mechanics 27: 503-517.

Wickert J A & Mote C D Jr (1991) Response and discretization methods for axially moving materials. Applied Mechanical Review, 44: 279-284.

Wickert J A & Mote C D Jr (1988) Current research on the vibration and stability of axially-moving materials. Journal of Shock and Vibration Digest 20: 3-13.

Wojak D B (1992) Acoustic and fluid structure interaction, a revision 5.0 tutorial. Swanson Analysis Systems, Inc. Houston.

Yue M G (1992) Belt vibration consideration moving contact and parametric excitation. International Power Transmission and Gearing Conference. ASME DE-Vol. 43-1.

Zaiser J N (1964) Nonlinear vibrations of a moving threadline. Ph.D. Dissertion, University of Delaware.

Zajaczkowski J & Lipinski J (1979) Instability of the motion of a beam of periodically varying length. Journal of Sound and Vibration 63: 9-18.

Zajaczkowski J & Yamada G (1980a) Further results of instability of the motion of a beam of periodically varying length. Journal of Sound and Vibration 68: 173-180.

Zajaczkowski J & Yamada G (1980b) Instability of a periodically moving plate. Journal of Sound and Vibration 68: 181-186.

Acceleration of a material particle in an axially moving membrane

The acceleration of a particle in a membrane can be developed in the same way as for a travelling cable in section 2.1.2. First, the change in velocity is expressed using the chain rule, a scalar version of equation (3.28), namely $\mathrm{d}\theta^{\alpha} = v^{\alpha}\,\mathrm{d}t$, and equation (3.34), i.e.

$$\begin{aligned} \mathrm{d}\,{}^{F}\mathbf{w} &= {}^{F}\mathbf{w}_{,\alpha}\,\mathrm{d}\theta^{\alpha} + {}^{F}\mathbf{w}_{,t}\,\mathrm{d}t \\ &= {}^{F}\mathbf{w}_{,\alpha}\,v^{\alpha}\,\mathrm{d}t + {}^{F}\mathbf{w}_{,t}\,\mathrm{d}t \\ &= \left(\mathbf{u}_{,ts} + \left[v^{\beta}\left({}^{I}\mathbf{a}_{\beta} + \mathbf{u}_{,\beta}\right)\right]_{,\alpha}\right) v^{\alpha}\,\mathrm{d}t \;+\; \left(\mathbf{u}_{,tt} + \left[v^{\beta}\left({}^{I}\mathbf{a}_{\beta} + \mathbf{u}_{,\beta}\right)\right]_{,t}\right)\mathrm{d}t\ . \end{aligned} \tag{A.1}$$

If we divide the change in velocity by dt, we obtain the acceleration vector in the form

$${}^{F}\mathbf{a} = \frac{\mathrm{d}\,{}^{F}\mathbf{w}}{\mathrm{d}t} = \mathbf{u}_{,tt} + 2\,v^{\alpha}\,\mathbf{u}_{,\alpha t} + v^{\alpha}\left[v^{\beta}\left({}^{I}\mathbf{a}_{\beta} + \mathbf{u}_{,\beta}\right)\right]_{,\alpha}\ . \tag{A.2}$$